



SAPIENZA
Università di Roma
Facoltà di Scienze Matematiche Fisiche e Naturali

PhD SCHOOL IN
CELLULAR AND DEVELOPMENTAL BIOLOGY

XXXI Cycle
(A.A. 2017/2018)

**A new cell labelling strategy to study the biogenesis
of exosomes and their role in human melanoma progression driven
by microenvironmental acidic pH**

PhD Student
Boussadia Zaira

Tutor
Prof. Giancarlo Poiana

Supervisor
Dr. Massimo Sargiacomo

Coordinator
Prof.ssa Giulia De Lorenzo

INDEX

SOMMARIO	5
SUMMARY	6
INTRODUCTION	7
AIMS OF THE WORK	11
RESULTS	13
1. BODIPY FL C₁₆ IS DISTRIBUTED IN ER/LATE ENDOSOMES REGIONS AND IS MAINLY METABOLIZED IN POLAR LIPIDS.	13
2. BODIPY-EXO PRESENTS DENSITY, MORPHOLOGY AND PROTEIN MARKERS CHARACTERISTIC OF EXOSOME.	18
3. BODIPY-EXO IMMUNOPRECIPITATION REVEALS EXOSOME- SPECIFIC PROTEIN MARKERS.	24
4. EXOSOME SECRETION STARTS WITHIN 5 MINUTES AND IS NOT AFFECTED BY TIME LABELLING.	25
5. BSA AND LOW TEMPERATURE INHIBIT EXOSOME INTERNALIZATION.	28
6. ENHANCED BODIPY-EXO SECRETION AT ACIDIC pH DEPENDS ON MELANOMA STAGE.	29
7. EXOSOME BIOGENESIS IS ENHANCED AFTER 1H OF pH TREATMENT.	33
8. ACIDIC EXOSOMES INDUCES MIGRATION AND INVASION IN MELANOMA CELLS.	35
9. ACIDIC EXOSOMES DISPLAY ENRICHMENT IN METABOLIC PATHWAYS RELATED TO TUMOR AGGRESSIVENESS.	38
10. ACIDIC EXOSOMES CONTENT MIRRORS PROTEIN EXPRESSION AT METASTATIC SITE OF MELANOMA PATIENTS.	42
DISCUSSION	47
MATERIAL AND METHODS	55
1. CELL LINES	55
2. CELL LABELLING	56

3. CELL TREATMENT WITH GW4869	56
4. EXOSOME ISOLATION	57
5. FLUORESCENT LABELLING OF EXOSOME PROTEINS	57
6. EXOSOME BIOGENESIS	58
7. FLOW CYTOMETRY ANALYSIS AND QUANTIFICATION OF EXOSOMES	58
8. LIPIDS EXTRACTION AND ANALYSIS	58
9. IODIXANOL DENSITY GRADIENT FOR VESICLES SEPARATION	59
10. EXOSOME LABELLING WITH ANTIBODIES FOR FC ANALYSIS	59
11. SDS-PAGE AND WESTERN BLOT ANALYSIS	60
12. ELECTRON MICROSCOPY.	61
13. IMMUNOPRECIPITATION.	62
14. CONFOCAL MICROSCOPY	62
15. MASS SPECTROMETRY ANALYSIS AND DATA PROCESSING	63
16. BODIPY-EXO TRANSFER AND FUNCTIONAL ASSAYS	65
17. META-ANALYSIS OF EXOSOMES MOLECULAR CARGO (PROGNOSCAN).	66
18. IMMUNOHISTOCHEMICAL STAINING	66
19. STATISTICAL ANALYSIS	67
REFERENCES	69
SUPPLEMENTARY MATERIAL	80
SUPPLEMENTARY REFERENCES	80
ABBREVIATIONS	82
LIST OF PUBLICATIONS	83

SOMMARIO

Gli esosomi sono nanovesicole di origine endosomiale, che rappresentano un mezzo importante di comunicazione cellula-cellula. Essendo coinvolti in diversi tipi di processi, sia fisiologici che patologici, sono diventati oggetto di sperimentazione clinica, nonostante molti meccanismi alla base della loro biogenesi rimangono tuttora sconosciuti. Quindi nel nostro laboratorio è stata messa a punto una metodica atta a produrre esosomi fluorescenti, in modo da poterne seguire la biogenesi nei diversi compartimenti intracellulari, il rilascio nell'ambiente extracellulare e la fusione con la membrana delle cellule riceventi. È stato quindi studiato, in un modello cellulare di melanoma umano, come questo precursore lipidico fluorescente è assorbito dalla cellula, accumulato all'interno del reticolo endoplasmatico, per poi diventare parte integrante della membrana degli esosomi. Queste nanovesicole fluorescenti sono state caratterizzate per dimensione, densità e presenza di marcatori proteici e successivamente è stata studiata con esperimenti di cinetica (5min – 24h) la secrezione. In seguito tale metodica è stata applicata allo studio della progressione del melanoma in condizioni di acidità microambientale. Nel melanoma è già noto che il pH microambientale è in grado di promuovere invasione e migrazione cellulare, e in questa tesi abbiamo analizzato il ruolo degli esosomi in tali processi. Quindi abbiamo studiato come cellule di melanoma umano, corrispondente a uno stadio intermedio, coltivate in ambiente acido producano una maggior quantità di esosomi, con un'aumentata capacità di trasferimento in cellule bersaglio. Inoltre queste vescicole presentano un profilo proteico che permette alle cellule riceventi di acquisire capacità migratorie e invasive. Infine, attraverso studi di meta-analisi ed *ex vivo* su biopsie di pazienti, è stato confermato che le molecole arricchite negli esosomi secreti in condizioni di acidità possano rappresentare dei marcatori della progressione del melanoma, convalidando quindi il valore diagnostico e prognostico degli esosomi.

SUMMARY

Exosomes, nanosized vesicles of endosomal origin, are worldwide recognized for their ability to transfer biological molecules, from cell to cell, crucial for both physiological and pathological processes. Hundred studies have been focused on exosome application also to clinics although biogenesis modalities are under investigation. Therefore, we set up a new effective fluorescent labelling strategy to trace exosome biogenesis and release with the aim to seek in human melanoma cell lines the impact that tumor progression may exert on their secretion and composition. Cells exposed to a fluorescent analogue of palmitic acid (Bodipy FL C₁₆) were able to promptly synthesize fluorescent phospholipids, constituents of exosome membrane bilayer. Afterwards, we were able to follow exosome biogenesis from the intracellular sites of origin to cell secretion, chasing over time by direct cytofluorimetric analysis.

To get insight into their function, we focused our studies on exosomes derived from melanoma cells maintained at low pH, which is a microenvironmental leverage for primary tumor to be transformed into widespread metastasis. When melanoma cells at specific intermediate stage were subjected to an acidic microenvironment, showed an increase in exosome release and transfer capability. Most importantly, when control melanoma cells were incubated with exosomes secreted in acidic medium acquired migratory and invasive capacities, demonstrating that exosomes carrying molecular payload can modify recipient cell program. Finally, meta-analysis and *ex vivo* studies confirmed the importance of acidic exosomes molecule content as marker of melanoma progression and so exosomes prognostic and diagnostic value.

INTRODUCTION

Extracellular vesicles are a heterogeneous group of cell-derived membranous structures. Depending on their biogenesis, they can be distinguished in exosomes, that originate from the endosomal compartment and have a range in size from 50 to 150 nm in diameter, and microvesicles, which are generated by the outward budding and fission of the plasma membrane and are 50-500 nm in diameter, but can be up to 1 μm (Colombo, Raposo and Théry, 2014; Tricarico, Clancy and D'Souza-Schorey, 2017). Exosomes are produced as IntraLuminal Vesicles (ILVs) within the endosome and are secreted in the extracellular space after the fusion of the MultiVesicular Endosome (MVE) with the plasma membrane (Harding, Heuser and Stahl, 1984; Pan *et al.*, 1985). Many different cell types are able to secrete membrane vesicles and this process is conserved throughout evolution, from bacteria to humans and plants (Deatherage and Cookson, 2012; Schorey *et al.*, 2015; Robinson, Ding and Jiang, 2016). An important machinery for exosome biogenesis is the Endosomal Sorting Complex Required for Transport (ESCRT) (Colombo *et al.*, 2013), which drive membrane shaping and scission after the clustering of ubiquitylated cargoes on microdomains of the limiting membrane of MVE (Hurley, 2008). This pathway can be then overlapped by syntenin and the protein ALG-2 interacting protein X (ALIX) (Baietti *et al.*, 2012). However, it has been described another subpopulation of exosomes that is generated in an ESCRT-independent manner, that requires the ceramide (Trajkovic *et al.*, 2008), formed by the neutral type II sphingomyelinase and the proteins of the tetraspanin family. Ceramide impose a negative curvature on membranes and is metabolised in sphingosine-1-phosphate to activate the G-protein-coupled receptor that seems essential for cargo sorting into ILVs. Tetraspanins can induce the inward budding of the microdomains in which they are enriched, thanks to their cone-like structure with an intramembrane

cavity that can accommodate cholesterol, and regulate the intracellular routing of cargoes (van Niel *et al.*, 2011). Therefore, most cells produce subpopulations of MVEs, with a heterogeneous content of ILVs, characterized by a different protein composition and morphology, and different mechanisms can act simultaneously or sequentially on MVE formation and specific cargo recruitment (Willms *et al.*, 2016).

The overlapping characteristics between the different types of vesicles, such as range of size and morphology, and the variable composition make difficult to distinguish them (Gould and Raposo, 2013; Kowal *et al.*, 2016). Even though the generation occurs at different sites within the cell, during biogenesis are involved common intracellular mechanisms and sorting machineries. In fact, even for exosomes and microvesicles, lipids and membrane-associated proteins are clustered in discrete membrane microdomains that are important both to participate in the recruitment of soluble components, that are then sorted into extracellular vesicles, and to promote membrane budding and fission for vesicles biogenesis and secretion (Van Niel, D'Angelo and Raposo, 2018). Furthermore, most common used isolation methods do not really allow a separation of the different kind of vesicles, as ultracentrifugation and purification based on antigen beads, which does not take into account vesicles heterogeneity and isolates only subpopulations (Colombo *et al.*, 2013; Colombo, Raposo and Théry, 2014).

Extracellular vesicles were first considered waste carriers, which were used by the cell to purge discarded elements, but nowadays they are considered an important mechanism for intercellular communication, capable to exchange components between cells (Cicero *et al.*, 2015; Rashed *et al.*, 2017). They can interchange protein, nucleic acid and lipid in both pathological and physiological conditions, acting as signalling vehicles for both short and long-range events (Simons and Raposo, 2009). In fact, it is now becoming increasingly clear that EVs mediate disease progression. Many cells have the ability to release exosomes whose composition and biogenesis vary depending on the physiological or pathological state of their cell of origin, and can be either influenced

by others stimuli (Théry, Zitvogel and Amigorena, 2002). Therefore, they are considered an important diagnostic tool for different pathologies, such as lactation, immune response and neuronal function (Admyre *et al.*, 2007), as well as implicated in pathological conditions such as liver diseases (Masyuk, Masyuk and Larusso, 2013), neurodegenerative diseases (Vella *et al.*, 2007) myocardial infarction (Li *et al.*, 2018) and cancer (Mathivanan, Ji and Simpson, 2010). Exosomes have been raised interest as potential source of disease biomarkers as well as to predict patient response to drugs, providing a tissue and cell type signature of the parental cells at the time of release since they are available in bodily fluids such as blood plasma, urine and saliva (Lane *et al.*, 2018; Momen-Heravi, Getting and Moschos, 2018).

For tumor progression and metastatization it is necessary a constant communication between cancer cells and the distant host environment. In this context, tumor-derived exosomes may contribute to this cross-talk by recruiting and reprogramming the tumor microenvironment (Kahlert and Kalluri, 2013). Tumor-derived exosomes have both pro- and anti-tumorigenic role in tumor progression. They can influence the tumor microenvironment by promoting angiogenesis or dysregulate immune surveillance in order to drive tumorigenesis (Greening *et al.*, 2015), but together they can be mediators of immune response against cancer cells, as described for melanoma (Hong *et al.*, 2016).

Cutaneous melanoma is one of the most aggressive cancers, with an increasing incidence. Its progression is related to genetic, epigenetic and environmental factors that lead to a stepwise malignant transformation of melanocytes, allowing their uncontrolled proliferation and the acquisition of invasiveness (Miller and Mihm, 2006). One of the principal cues of progression is the microenvironmental acidification, that is the consequence of an upregulated glycolysis, so that the local microenvironment in human melanoma has been reported to be at pH between 6.4–7.3 (Wike-Hooley, Haveman and Reinhold, 1984). In the early phases, extracellular acidity influences tumor gene expression by up modulation of several genes encoding receptors, signal proteins, transcription factors, cytokines (Fukamachi *et al.*, 2013), involved in

invasion, tissue remodeling, cell cycle control and proliferation (Rofstad *et al.*, 2006; Moellering *et al.*, 2008), thus leading to a more malignant cell phenotype.

Melanoma cells have a high propensity to spread to distant sites, so that the prognosis is generally poor (Aubuchon *et al.*, 2017). Both tumour expansion and the development of metastasis are regulated by the cross-talk between cancer cells and the surrounding stromal components (Palmieri *et al.*, 2015). This mechanism is mediated by exosomes, that are secreted by normal as well as malignant cell populations and drive many specialised functions implicated in intercellular signalling, protein cargo transport, proliferation, cancer development (Vlassov *et al.*, 2012) and degradation of extracellular matrix by metalloproteases (Hakulinen *et al.*, 2008; You *et al.*, 2015). Moreover exosomes secreted by melanoma cells are able to migrate toward distant tissue to prepare the pre-metastatic niche (Peinado *et al.*, 2012, 2017) and their fusion with their target cells prepare recipient tissue so that it becomes permissive for the subsequent homing of metastatic cells (Hoshino *et al.*, 2015).

The identification of predictive and prognostic biomarkers in cancer is an active area of research, but thus far only few molecules are relevant for clinical application. However, recent studies have proposed the use of exosomes in cancer for diagnostic and prognostic purposes, in a non-invasive strategy. Indeed, these vesicles may represent a useful tool for characterization of the melanoma molecular signature (Tucci *et al.*, 2018).

AIMS OF THE WORK

The aim of this study was firstly to elucidate the kinetic of exosome biogenesis and release, and to better characterize these vesicles. At the present time, the biochemical characterization and purification of exosomes from the entire population of extracellular vesicles remains a challenging investigative issue, only partially solved (Nolte- *et al.*, 2012; Cicero *et al.*, 2015; Kowal *et al.*, 2016). Microvesicles (MV) and Exosomes (Exo) are similar in physical properties, as size and floating density, or in intrinsic characteristics, as molecular content. Thus, they can be easily mixed up once co-present in secretory fluids (Record *et al.*, 2014; Kreimer *et al.*, 2015). Therefore, to monitor the traffic of the entire exosome population we developed in our lab an innovative methodology based on the use of a fluorescent fatty acid analogue, BODIPY FL C₁₆ (Bodipy C₁₆), which is metabolized by the cell and generates the majority of phospholipids species, mainly directed in the endosomal compartment (Coscia *et al.*, 2016). This lipid precursor enables to follow the kinetic of exosome release and of their uptake by target cells. Moreover, we aim to apply this new effective strategy for the isolation of a specific population of exosome from the bulk of extracellular vesicles, with the purpose to clearly characterize these vesicles and their biogenesis within the cell.

Notably, this method represents an improvement on exosomes Flow Cytometry-based studies so far reported, and provides a quantitative correlation between exosome uptake and cell functional effects.

Then, by means of this procedure, we studied the role of exosomes in melanoma progression, driven by acidic microenvironmental pH, and as a function of tumor stage. To this aim we developed an *in vitro* model based on human melanoma cell lines representative of various steps of melanoma progression, cultured at acidic pH ranging between pH 6.0-6.7 (WARBURG, 1956; Helmlinger *et al.*, 1997). In fact, the extracellular pH in the *core* regions of tumors decreases to pH 6.7 and below because of lactate accumulation (Vaupel, Kallinowski and Okunieff, 1989;

Helmlinger *et al.*, 1997).

It has been previously described that the increase in the amount of secreted exosomes represents a hallmark of disease stage progression (Logozzi *et al.*, 2009; Alegre *et al.*, 2014), so we hypothesize that, since acid pH is known to be a microenvironmental leverage for primary tumor to be transformed into widespread metastasis, the cell responsiveness to acidic pH could result in an enhanced exosome secretion.

However, since a role of exosomes, secreted in a microenvironmental acidic condition, in promoting melanoma progression was not described so far, we studied if exosomes alone are able to induce in control target cells the acquisition of new migratory and invasive capabilities. This ability highlights the importance of exosome content as the summary of the necessary pathways responsible for tumor progression. Therefore, we will analyse the vesicles protein profile and some proteins, that are upregulated in acid exosomes, will be checked in *ex vivo* assay as biomarkers of melanoma advancement.

Altogether, the results of these experiments will provide an innovative technology to study exosome role in different biological processes and, in particular, in this study we will be able to detect key molecules involved in melanoma aggressiveness, which could be the object of new therapeutic and diagnostic strategies.

RESULTS

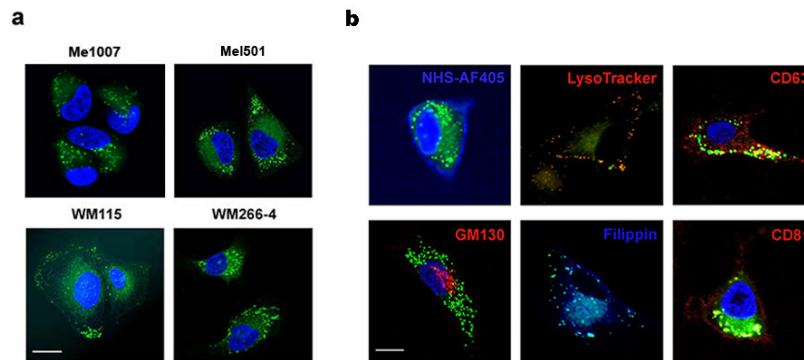
1. Bodipy FL C₁₆ is distributed in ER/late endosomes regions and is mainly metabolized in polar lipids.

To get insight into the intracellular distribution of Bodipy C₁₆, we first evaluated cell fluorescence in four human melanoma cell lines. After 2 hours Bodipy C₁₆ uptake, confocal microscopy images of all tested cell lines showed similar fluorescence distribution, likely restricted in the Endoplasmic Reticulum (ER)/late endosomal/MultiVesicular Body (MVB) compartments (Fig. 1a), and was not detected in the plasma membrane.

To better characterize the subcellular localization of Bodipy C₁₆ we performed confocal microscopy analysis (Fig. 1b) using LysoTracker, a probe for acidic organelles/lysosomes, and Filipin, a probe for free non-esterified cholesterol that has been shown to label the recycling endosome area but not lipid droplets (Maxfield and Wüstner, 2012). Furthermore, colocalization with the Exosomal/MVB markers CD63 and CD81 highlighted that Bodipy C₁₆ preferentially labels ER/late endosomal compartments. Remarkably, fluorescence seemed completely absent from the plasma membrane, labelled with the membrane impermeable protein reagent NHS-AF405, or from the cis-Golgi, labelled by GM130 (Demers *et al.*, 2015).

These results strongly suggest that Bodipy C₁₆ allows for the identification of defined sub cellular compartments (supposedly ER and endosomes) involved in Exo biogenesis.

Figure 1

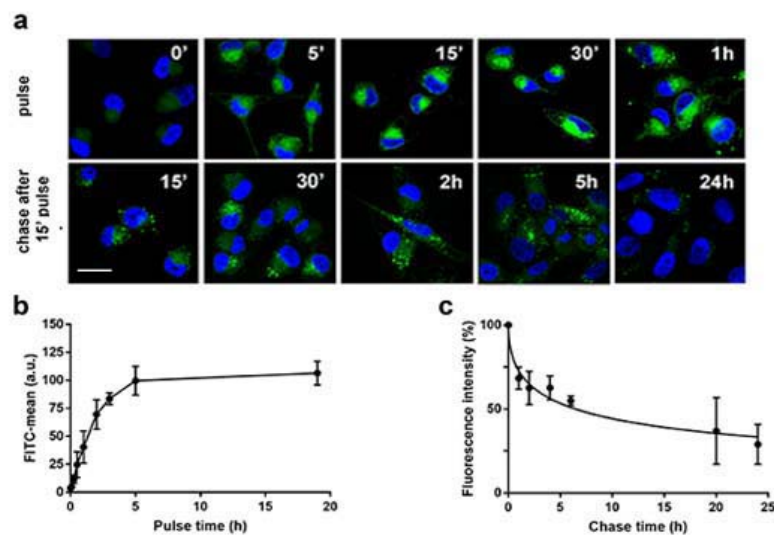


Bodipy FL C₁₆ is distributed in the ER and endosome region. (a) Confocal microscopy images of a panel of differently staged human melanoma cell lines, labelled with Bodipy C₁₆ for 2 hours. **(b)** Colocalization of Bodipy C₁₆ with specific organelle markers after a 2 hours pulse with Bodipy C₁₆. Images are representative of at least two independent experiments. All scale bars indicate 20 μ m.

To study the cellular transport kinetics of Bodipy C₁₆ through the endo/lysosomal compartment, we performed pulse-chase experiments. Cells were pulsed with Bodipy C₁₆ for different times, or pulsed for 15 min and chased for different times up to 24 hours (Fig. 2a). The fluorescent probe is taken up by cells very rapidly, just after 5 min, and its uptake increases during pulse times. The fluorescence is rapidly localized in perinuclear ER areas and becomes more and more concentrated in specific regions, likely corresponding to late endosomal/MVB compartments. During chase times, spots fluorescence increases his intensity and after 24 hours is mostly chased out. To quantify the Bodipy C₁₆ uptake and metabolism, we pulsed and chased cells for different times and measured cell fluorescence by Flow Citometry (FC) (Fig. 2b-c). The probe uptake, in Mel501 (MNI) cells, reached saturation after 5 hours (Fig. 2b), which has been since chosen

for cell labelling. During chase times in fresh medium (Fig. 2c), we observed after 1 hour a drastic reduction of cell fluorescence to about 30% of initial values that reaching 50% in 6 hours and slowly decreasing afterwards.

Figure 2

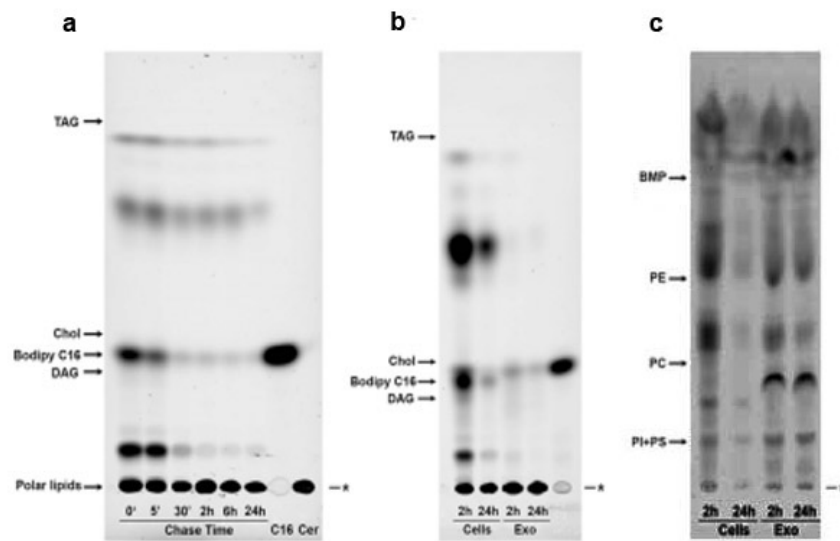


Pulse-chase experiments of cells labelled with Bodipy C₁₆ and total lipid analysis. (a) Confocal microscopy analysis of MNI cells pulsed for different times with Bodipy C₁₆ (upper panel) or pulsed for 15' and chased for different times in complete medium (medium panel). Scale bar indicates 20 μ m. Data are representative of at least three independent experiments. (b) Cells were treated with Bodipy C₁₆ for the indicated amount of time (c) or treated for 15 minutes, washed and chased in complete medium. Cell fluorescence was analysed by FC. Data are expressed as mean \pm SEM (n = 3).

To determine how the Bodipy is metabolized, and to be sure that there is no more free probe, we performed High Performance Thin Layer Chromatography (HPTLC). We first analysed cells at different chase times (Fig. 3a), and found that the fatty acid analogue is metabolized in polar lipids just after the end of pulse time, and the presence of free probe decrease during chase. Interestingly, Bodipy is not metabolized in triglycerids (TAG) and cholesterol (Chol), highlighting that the labelling is not attributable to lipid droplets. Next, we analysed fluorescent lipids in exosomes isolated after 1 hour or 24 hours of chase time (Fig. 3b), to ensure that fluorescence was associated to vesicles with metabolized phospholipids, and not to lipid probe aggregates. We found that pelleted exosomes are mainly composed by fluorescent polar lipids and there is negligible free probe. Moreover we checked the actual transformation in cell major phospholipid classes, both in cells and exosomes, at 1 hour and 24 hours of chase time (Fig. 3c). We found the presence of phosphatidylinositol (PI), phosphatidylserine (PS), phosphatidylethanolamine (PE), and most importantly bis(monoacylglyceryl)phosphate (BMP), a lipid previously described to be important for exosome biogenesis and found enriched in these vesicles (Record *et al.*, 2014).

This data suggest that cells internalize Bodipy C₁₆, that arises a plateau at 5 hours, and is transported to the endoplasmic reticulum were it is metabolized mainly in phospholipids. Then, the probe is directed to the endosomal pathway and becomes part of the exosome membrane.

Figure 3



Total lipid analysis of Bodipy C₁₆ labelled cells and exosomes. (a) Cells were pulsed with 7 μ M Bodipy for 15' and chased for different times (0', 5', 30', 2h, 6h, 24h). Total lipids were extracted from 500.000 cells and then neutral lipids were separated by HPTLC, using the appropriate solvent mixture. (b-c) MNI cells were pulsed with 7 μ M Bodipy for 5h and chased for 2h and 24h. Exosomes were isolated from cell culture supernatant at 1h chase time and, after addition of fresh medium to the same flask, at next 24h. Lipids were extracted and 40.000 cells and $8,6 \times 10^6$ exosomes for each chase time point were separated by HPTLC for (b) neutral lipids and (c) phospholipids. Data are representative of at least three independent experiments.

2. Bodipy-Exo presents density, morphology and protein markers characteristic of exosome.

This innovative methodology enables the fluorescent labelling of exosomes, which can thus be easily analysed by Flow Cytometry (FC). Bodipy C₁₆ is metabolized by the cell and transformed into principal exosome membrane lipids, thus vesicles can be counted and fluorescent population distribution can be visualized, enabling exosome tracing and characterization.

As it has been described that in hepatocyte cell lines treatment with Palmitic acid alters exosome production (Lee *et al.*, 2017), to be sure that visualized vesicles were not an artefact produced by the fluorescent fatty acid, we compared exosomes isolated from untreated cells, Bodipy C₁₆-treated cells, and Palmitic acid-treated cells. Total pelleted vesicles were run on a 10% SDS-PAGE gel and analysed for the main exosomal protein markers (Fig. 4a). We found that there are no differences among the three conditions; so we can infer that produced vesicles were not the result of any treatment, but represented the physiological production of this melanoma cell line.

Conversely, for protein characterization and visualization, we labelled Bodipy-Exo with Alexa Fluor 647 NHS Ester, a water-soluble far-red dye that labels proteins on the external surface of vesicles (C16/AF647 Exo). After labelling, fluorescent exosomes were loaded on top of a continuous iodixanol density gradient and twelve fractions were collected and analysed by FC (Fig. 4b). An equal volume of each fraction was precipitated using trichloroacetic acid (TCA) and run on a 10% SDS-PAGE gel that was fixed and scanned on a Thypoon 9500 laser scanner (Fig. 4c). The fluorescent protein pattern, corresponding to EVs external proteins, shows a specific profile for each fraction. Interestingly, fluorescent exosomes are enriched in fraction 4, which has a density of 1.07 – 1.09 g/mL, slightly lower than what described (Willms *et al.*, 2016), and which presents a more heterogeneous protein profile. Western blot analysis, for the presence of exosome markers Flotillin-1, TSG101 and CD81 (Fig. 4d), showed their presence in fractions corresponding to

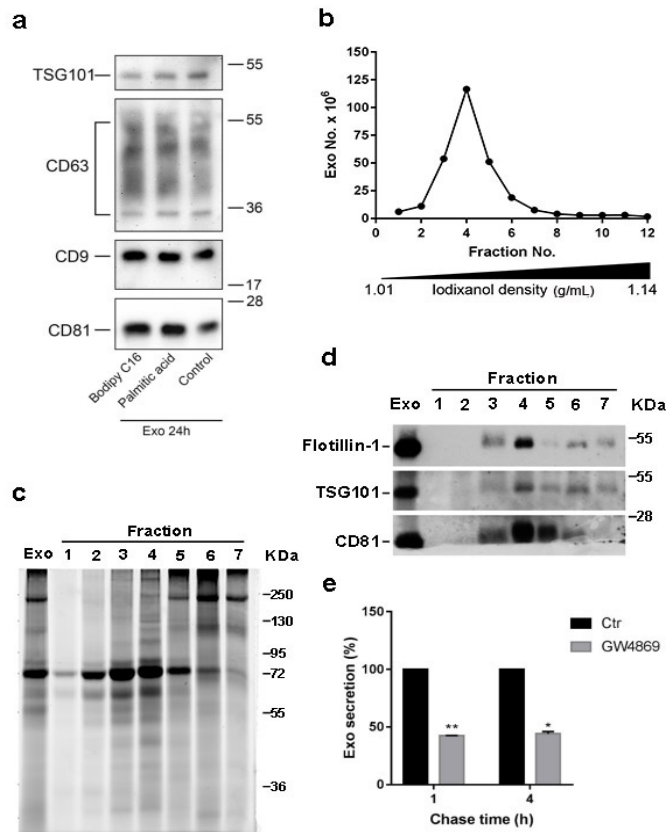
the Bodipy-Exo fluorescent peak. Notably, TSG101 and Flotillin-1 are present in additional fractions non-corresponding to the fluorescent exosome peak. This is in agreement with experiments carried out in other cell models (Willms *et al.*, 2016), showing that cells may secrete different subpopulations of exosomes with diverse densities. In addition it is well established that ultracentrifugation and density gradient does not allow a complete separation of vesicles of different origin, resulting in the presence of markers that might be exosome specific or not.

Moreover, to further characterize exosome population and to investigate if fluorescent vesicles biogenesis is ceramide-dependent, we treated MNI cells with GW4869 (Fig. 4e), the neutral sphingo-myelinase (nSMase) inhibitor, described to reduce exosome release (Trajkovic *et al.*, 2008; Cheng *et al.*, 2017). In fact, we found that there is a significant decrease of exosome secretion by approximately 50%, both at 1h and at 4h of chase time.

Therefore, we can infer that fluorescent vesicles described so far are attributable to exosome of endosomal origin, generated, at least in part, by a ceramide-dependent pathway.

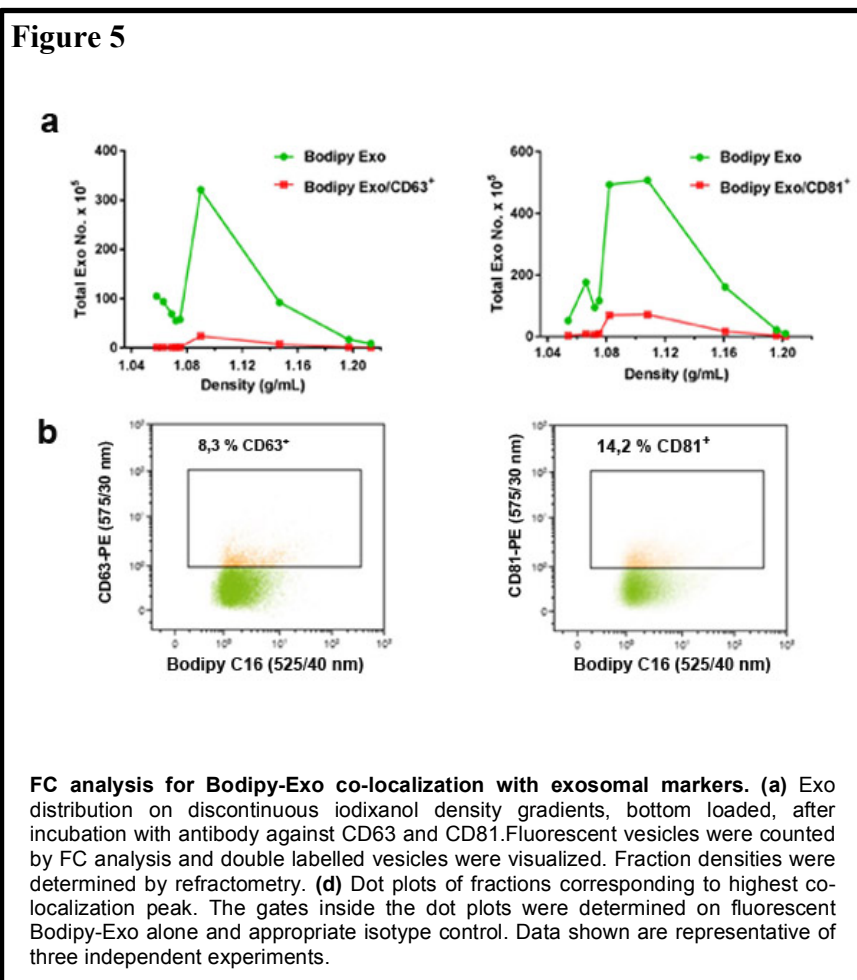
To confirm the co-expression of exosomal markers on Bodipy-Exo, we marked fluorescent exosomes with anti-CD81, anti-CD63 PE-conjugated antibodies and further separated double-labelled exosomes by upward flotation into discontinuous iodixanol density gradients. This last purification step was performed to separate the labeled EVs from unbound antibodies, which interfere in the FC analysis (Kormelink *et al.*, 2016). Fractions were analysed by FC for Bodipy-Exo count and co-staining with fluorescent antibodies (Fig. 5a). Bodipy-Exo as well as CD81 or CD63 positive Bodipy-Exo regularly floated in a discrete peak ranging from densities of 1,08-1,15 g/mL, consistent with the density range classically reported for Exo (Colombo, Raposo and Théry, 2014), and slightly higher than what observed with top loaded density gradients. Double-labelled Bodipy-Exo with CD63 and CD81 were 8 % and 14 % respectively (Fig. 5b) with respect to the total Bodipy-Exo.

Figure 4



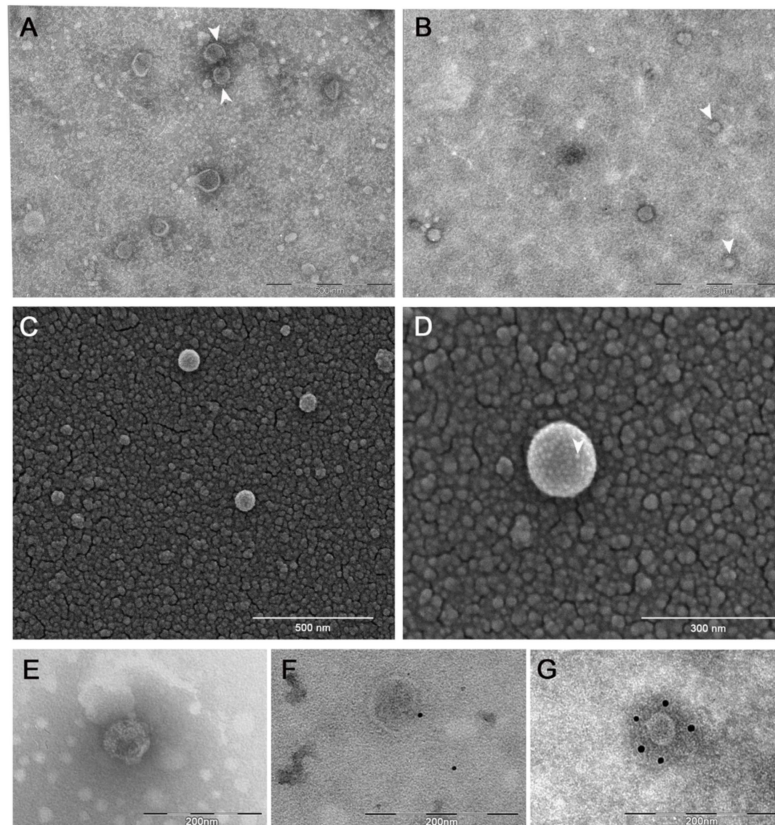
Fluorescent Exosome characterization. (a) Melanoma cells were treated with Bodipy C₁₆, or Palmitic acid or left untreated for 5h at 37 °C, washed and incubated with complete medium. After 24h conditioned medium was recovered for vesicles isolation. Total collected vesicles were loaded on a SDS-PAGE gel for Western blot analysis with antibodies specific for TSG101, CD63, CD81 and CD9. (b) Bodipy-Exo were loaded on top of a continuous iodixanol density gradient (5-35%) and subjected to ultracentrifugation for 16 h at 100.000 x g in SW60 rotor. The resulting fractions (1–12) with increasing density were analysed by FC for Exo count. Fraction density were checked by refractometry. (c) Fractions from 1 to 7 were loaded on SDS-PAGE gel, which was scanned on a gel scanner for the analysis of fluorescent proteins pattern. (d) The presence of Exo protein markers Flotillin-1, CD81 and TSG101 was analysed by Western blotting using an equal volume of each sample. Data shown are representative of three independent experiments. (e) Bodipy-Exo were isolated from Mel501 cells pre-treated or not with GW4869 for 19h, pulsed with Bodipy C₁₆ and cultured for 1h and 4h in the absence or presence of 10 μM GW4869. Isolated fluorescent vesicles were counted by FC. All data are expressed as mean ± SEM (n = 3).

Therefore, this data confirms that fluorescent vesicles contains proteins specific of exosomes. However, the low rate of expression of the two protein markers shows the heterogeneity of exosome population, probably depending on their differential biogenesis pathway. In fact, it has recently been described that exosomes represent a heterogeneous population with different expression of the typical protein markers, such as CD63, CD9, and CD81 tetraspanins (Kowal *et al.*, 2016).



Moreover, to further confirm that Bodipy-Exo are membrane vesicles and not protein aggregates or non-membranous particles, we performed electron microscopy analysis of 100.000 x g ultracentrifugation pellet deriving from untreated (Fig. 6a) or Bodipy C₁₆ treated (Fig. 6b) cells. Electron microscopy images of the two negatively stained samples show a homogeneous mixture of vesicles with the typical exosome morphology and size (30-150 nm). Notably, some vesicles display protein spikes that protrude from membrane bilayer (white arrowhead). Scanning electron microscopy (SEM) of Bodipy-Exo shows a tri-dimensional view of these vesicles, confirming the average diameter of this purified exosome population (Fig. 6c-d) and the protrusion of external proteins on the surface (white arrowheads). However, TEM analysis of the Bodipy-Exo population purified by iodixanol density gradient has demonstrated that fractions comprising the fluorescent peak quite exclusively contains vesicles with the typical exosome size (Fig. 6e). Importantly, immunogold labelling of exosomes with antibody against Bodipy FL shows a poor gold signal of the fluorescent vesicles, probably due to the difficult antigen access (Fig. 6f), but confirming that fluorescent population is represented by vesicles with property and size characteristic of described exosomes. Moreover, anti-CD81 antibodies easily recognize proteins around the exosome surface (Fig. 6g), validating that analyzed vesicles have the typical exosome protein composition.

Figure 6

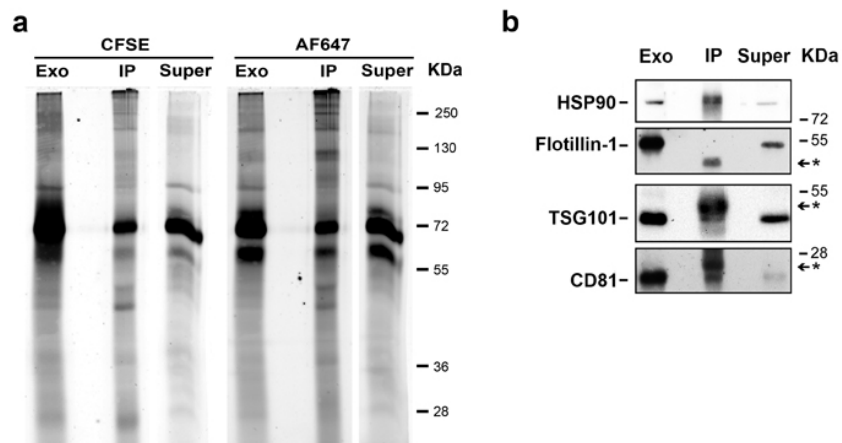


Transmission and Scanning Electron Microscopy analysis of Exosomes. Negative staining of exosomes from MNI cells labelled (b) or not (a) with Bodipy C₁₆. (c) SEM analysis of Bodipy-Exo. (d) SEM micrograph at high magnification (300k) of a Bodipy-Exo. (e) Negative staining of iodixanol density gradient fractions containing fluorescent exosome peak (f) Immunogold labelling of Bodipy-Exo with rabbit anti-bodipy antibodies and 10nM gold conjugated anti-rabbit IgG antibodies. (g) Immunogold labelling of Bodipy-Exo with mouse anti-CD81 antibodies and 10nM gold conjugated anti-rabbit IgG antibodies.

3. Bodipy-Exo immunoprecipitation reveals exosome-specific protein markers.

We tested the possibility to immune-isolate Bodipy-Exo by using an anti-Bodipy FL specific antibody. This approach allowed us to separate a selected population of metabolically labelled exosomes and analyse them by Western blot. SDS-PAGE gels of immunoprecipitated Exo and supernatants were also scanned for fluorescence, either in the green channel for CFSE labeled proteins or in the red channel for AF647, to distinguish on a qualitative level between external (NHS-AF647) and internal (CFSE) exosome proteins (Fig. 7a). Bodipy-Exo or double labelled C16/AF647-Exo were immunoprecipitated with similar efficiencies (about 65%), showing that NHS-AF647 labelling does not affect antibody recognition of fluorescent lipids. Results indicate a distinct fluorescent proteins profile of immunoprecipitated Exo with respect to total Exo for either CFSE or NHS-AF647 labelling. Importantly, CFSE labelling confirms that Bodipy-Exo represent a population of protein-loaded vesicles. However, we found that there is just a slightly difference between external and internal protein profile, being most of exosome proteins present on the membrane. Western blot analysis showed the presence of classical Exo markers (Fig. 7b), such as HSP90, TSG101 and CD81 but remarkably not Flotillin-1 (Kowal *et al.*, 2016), a marker of EV not Exo-specific but present in total exosome fractions. Therefore, this new approach can be useful to determine the exosome specific markers and the purification of vesicle of endosomal origin, without the contamination of other type of extracellular vesicles.

Figure 7



Fluorescent exosome immunoprecipitation reveal exosome-specific protein markers. Immunoprecipitation was performed as described using an antibody against Bodipy FL. **(a)** Pelleted vesicles were treated with CFSE and NHS-AF647 for 30 min before immunoprecipitation. Green and red fluorescent proteins of total vesicles were run on a SDS-PAGE gel and analysed with a gel scanner. Data shown are representative of three independent experiments. **(b)** Exosomes recovered from conditioned medium after 24h chase were immunoprecipitated using antibody against Bodipy FL. Both immunoprecipitated and immunoprecipitation supernatants were loaded on a SDS-PAGE gel for Western blot analysis with antibodies specific for Flotillin-1, CD81, TSG101 and HSP90. Total Exo were used as positive control. Nonspecific signal from the immunoglobulins' heavy (50 kDa, Tsg101 and Flotillin-1 blot) or light (25 kDa, CD81 blots) chains used for immunoprecipitation are indicated (*).

4. Exosome secretion starts within 5 minutes and is not affected by time labelling.

Finally, to determine the timing of exosome biogenesis, and if different labelling time could affect the kinetic of exosome secretion, we pulsed and chased cells at different times.

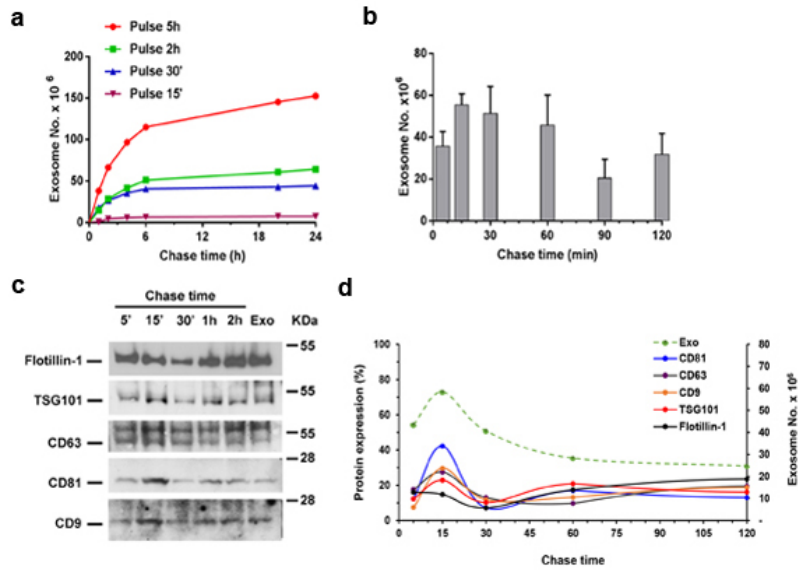
Firstly, we pulsed cells with Bodipy C₁₆ for 15 min, 30 min, 2 or 5 hours, washed and chased cells in fresh medium. At different time points,

culture medium was harvested, for Exo isolation, and fresh medium was added to the same flask (Fig. 8a). The kinetic of Exo release is the same, independently of the pulse times, and reaches a plateau at 6 hours, but the amount of secreted Exo is dependent on the initial load of Bodipy C₁₆ within the endosomal compartment.

Since most of the fluorescent exosomes are secreted in the first hours of chase time, we sought to determine if we could define the time needed for Bodipy-Exo release (Fig. 8b). We then pulsed cells with Bodipy C₁₆ for 5 hours and harvested conditioned medium at different time points, as described for previous experiments. Interestingly, we found that the majority of exosomes is secreted in early times, suggesting that vesicles secretion during chase time is immediate.

Exo released at different time intervals were analysed by Western blot (Fig. 8c), for the presence of major exosome protein markers. Densitometric analysis of protein bands (Fig. 8d) demonstrates that the intensity pattern follows the trend of Bodipy-Exo release. In particular, Exo markers as CD81 and CD63 are more abundant at 15 minutes, when Bodipy-Exo release reaches the highest peak. On the contrary, Flotillin-1, an EVs marker not specific for Exo (Colombo, Raposo and Théry, 2014), seems to increase over time, when Bodipy-Exo secretion decreases but probably EVs heterogeneity rises.

Figure 8



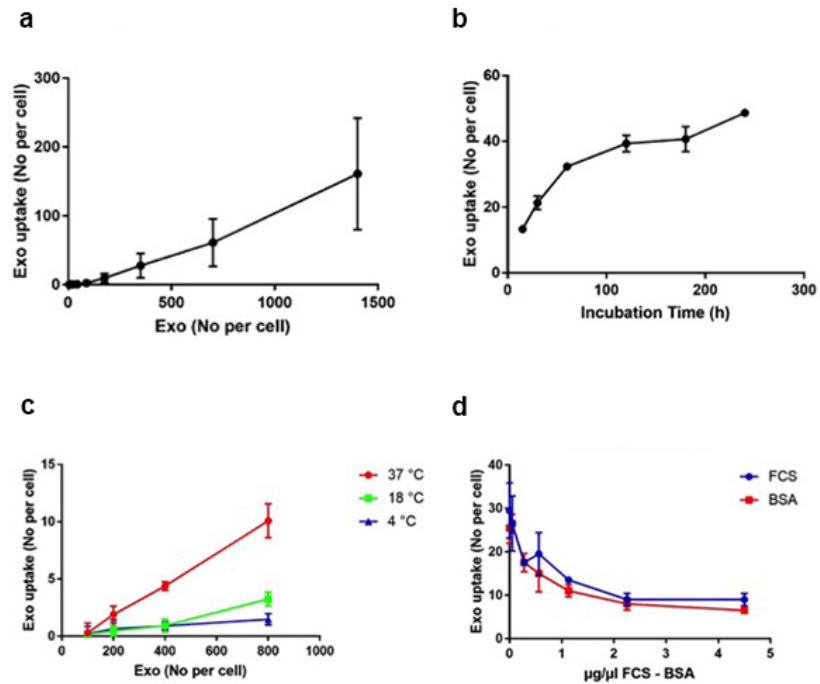
Exo biogenesis and release kinetic (a) Cells were pulsed with Bodipy C₁₆ for different times, washed and chased in fresh medium. At the indicated time points, conditioned medium was harvested and amount of secreted Bodipy-Exo determined by FC. Data at each time point is the sum of Exo secreted in the interval between each wash/fresh medium addition. Data shown are representative of three independent experiments. **(b)** The amount of secreted Exo at different time intervals after a 5 hours pulse with Bodipy C₁₆. Data are expressed as mean \pm SEM (n = 4) **(c)** Exo secreted at different time points were run on a SDS-PAGE gel, blotted and probed with antibody against Exo markers. Equivalent volumes of each sample were loaded on the gel. Exo, secreted after 24h of chase time were used as positive control. **(d)** Densitometric analysis of the expression of tested proteins. For each protein, data are showed as percent of expression relative to the total of the density of all samples. The green line (Exo) represent the amount of Exo secreted at different time points.

5. BSA and low temperature inhibit exosome internalization.

Bodipy C₁₆ labelling enables the quantification of exosome uptake in target cells, by FC analysis. We first performed a study about exosome internalization, with dose-response (Fig. 9a) and time-course (Fig. 9b) experiments, incubating fluorescent exosomes with untreated cells, and analysing the increase of cell fluorescence. Then, we found the suitable concentration and time for exosome incubation, which consists in 700 exo/cell and 2 hours. Taking into account these two conditions, we analysed how exosomes internalization can be inhibited.

The study of the interaction between exosomes and FCS is important because it is already known that these vesicles are enriched in the bloodstream to reach distant target cells (Peinado *et al.*, 2012). Therefore, we were interested in understanding how serum affects exosome uptake. We performed different experiments, to study the effects of temperature (Fig. 9c), Bovine Serum Albumin (BSA) and Fetal Calf Serum (FCS) (Fig. 9d). In temperature dependent uptake experiments we found that both 18 °C and 4 °C temperature decrease the number of exosomes internalized per cell, in accordance with the block of endocytosis (Punnonen, Ryhanen and Marjomaki, 1998; Suesca *et al.*, 2013). We found that FCS decreases exosome internalization into cells and, interestingly, we can speculate that most of this inhibitory effect can be attributable to albumin.

Figure 9



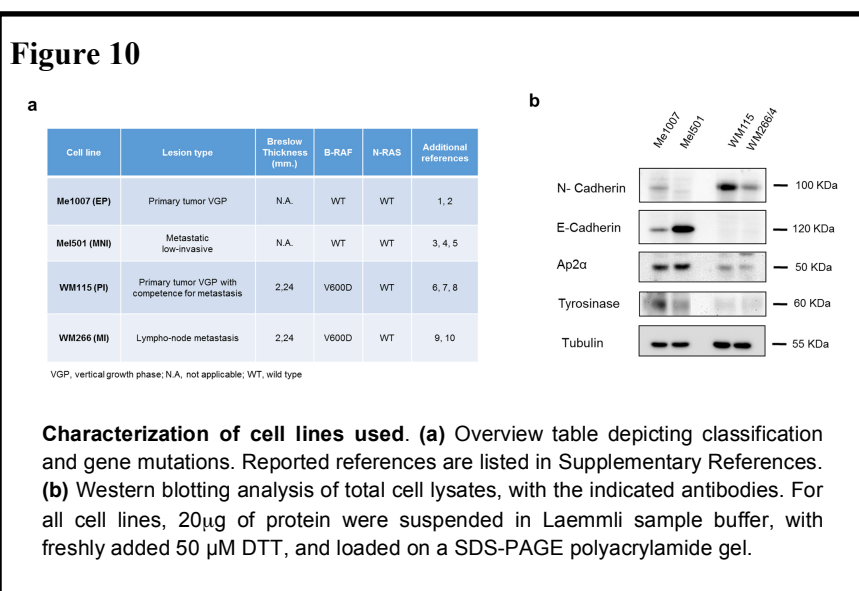
Exosome internalization is inhibited by BSA and low temperature. (a) Dose-response, **(b)** Time dependent, **(c)** Temperature dependent and **(d)** Inhibition uptake of Bodipy-Exo on Mel501 cells. 30.000 cells were incubated with **(a)** increasing amount of exosomes or with 700 Bodipy-Exo per cell for **(b)** different time, or **(c)** different temperature, diluted in HANK's buffer. Otherwise **(d)** cells were incubated with 700 exo per cell for 1 hour in medium containing different concentration of FCS or BSA. At the end of incubation, cells were analysed by FC for fluorescence. Data are expressed as mean \pm SEM (n = 4).

6. Enhanced Bodipy-Exo secretion at acidic pH depends on melanoma stage.

We applied this methodology to decipher unknown steps of melanoma progression. Thus, we developed a model based on a panel of differently

staged human melanoma cell lines, and evaluated the influence of acidic pH microenvironment on tumor progression. Melanoma can grow in a context of extracellular acidosis within the range of pH6.4 to 7.3 (Wike-Hooley, Haveman and Reinhold, 1984; Vaupel, Kallinowski and Okunieff, 1989). To mimic *in vitro* the action of tumor microenvironment, we cultured different human melanoma cell lines in acidified media at pH 6.7 and pH 6.0.

To better define the stage of the melanoma cell lines used, we summarized the classification and gene mutations (Fig. 10a), and evaluated whether molecules related to melanoma progression, such as E-, and N-cadherin, involved in epithelial-mesenchymal transition (EMT), Tyrosinase and AP2 α were differently expressed (Fig. 10b). Results indicated the occurrence of EMT together with expressions of AP2 α and Tyrosinase in Primary Invasive (PI: WM115) and Metastatic Invasive (MI: WM266-4) cells, in line with an advanced tumor stage. On the contrary, Early Primary (EP: Me1007) and Metastatic not Invasive (MNI: Mel501) being in a pre-EMT phase, showed a higher expression of AP2 α and Tyrosinase, thus indicating an earlier phase of tumor progression.



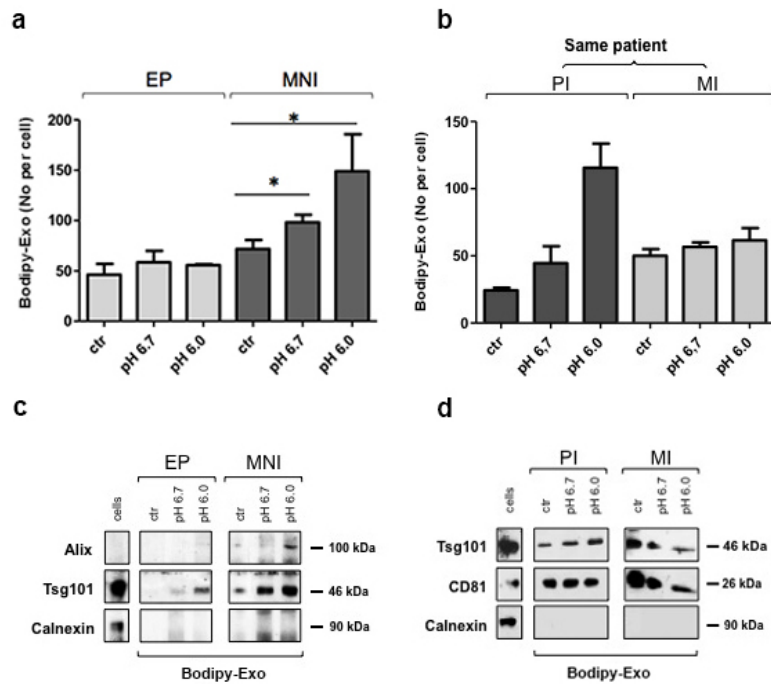
We labelled both MNI and EP melanomas with fluorescent probe, and analyzed them by confocal microscopy. After 24 hours incubation, either at neutral (ctr) or acidic pHs (pH6.7 or pH6.0), cell fluorescence appeared either diffuse in the endoplasmic reticulum area or restricted in spots (Fig. 11c).

Then, to study the amount of secreted exosomes, on the basis of disease stage, and to reveal how exosome release by melanoma cells can be influenced by acidic pH, we used the above-described strategy by comparing Bodipy-Exo secretion either in EP and MNI, as well as in the PI and MI melanomas, deriving from the same patient.

Bodipy-Exo were recovered from melanoma cell lines cultured at pH 6.0 and 6.7 for 24 h and FC counted. The acidity of the medium significantly enhanced exosome secretion when compared to buffered medium (ctr) in MNI, but not in EP melanomas (Fig. 12a). One explanation might be that the acidic treatment does not influence exosome secretion in early primary melanomas due to their intrinsic scarcely aggressive nature.

Secreted exosome count conducted on PI and MI cell lines confirmed the higher exosome secretion in advanced versus primary melanomas. Specifically, in standard culture condition MI produced 50 exosome per cell versus 25 secreted by PI, in line with its more aggressive nature (Fig. 12b). However, in this case, acidic pH positively influenced exosome release in primary, but not in metastatic cell lines, thus suggesting that it can influence exosome secretion at a specific tumor developmental stage, i.e. only when the massive secretion of specific molecules is required for the spread of the tumor and the progression of the disease. Accordingly, PI resulting pH-sensitive, is already endowed with invasive capability, thus indicating a more advanced stage with respect to EP not responsive to acidic pH in terms of exosome release. The identity of these vesicles as exosomes was confirmed by the expression of the common exosome markers Tsg101, Alix and CD81 and the absence of calnexin (Fig. 12c,d) (Lötvall *et al.*, 2014).

Figure 12

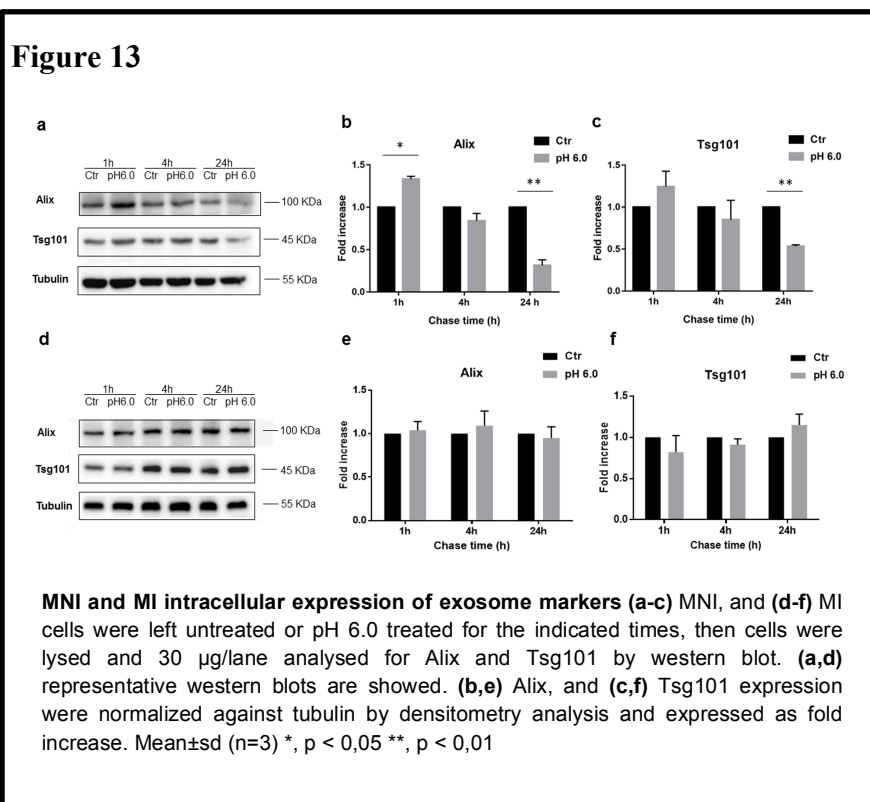


Bodipy-Exo secretion is affected by acidic (pH6.0 and pH6.7) treatment only in intermediate melanoma cell lines. EP, MNI, (a) PI and MI (b) cells were treated with C_{16} ($7\mu\text{m}$) for 5h and then cultured in control or acidic (pH6.0 or pH6.7) medium for 24h. Hereafter conditioned medium was subjected to ultracentrifugation for exosome isolation. Fluorescent vesicles were then counted by FC. The graph shows the number of secreted Bodipy-Exo per cell. (c,d) Western blot analysis of total isolated vesicles for the presence of principal exosome markers (Alix, Tsg101 and CD81) and the absence of Calnexin, a marker of ER used as a negative control. Data shown are representative of three independent experiments. * $p < 0.05$.

7. Exosome biogenesis is enhanced after 1h of pH treatment.

To investigate a potential trigger to enhanced exosome secretion we first evaluated intracellular exosomal markers expression (Alix and Tsg101)

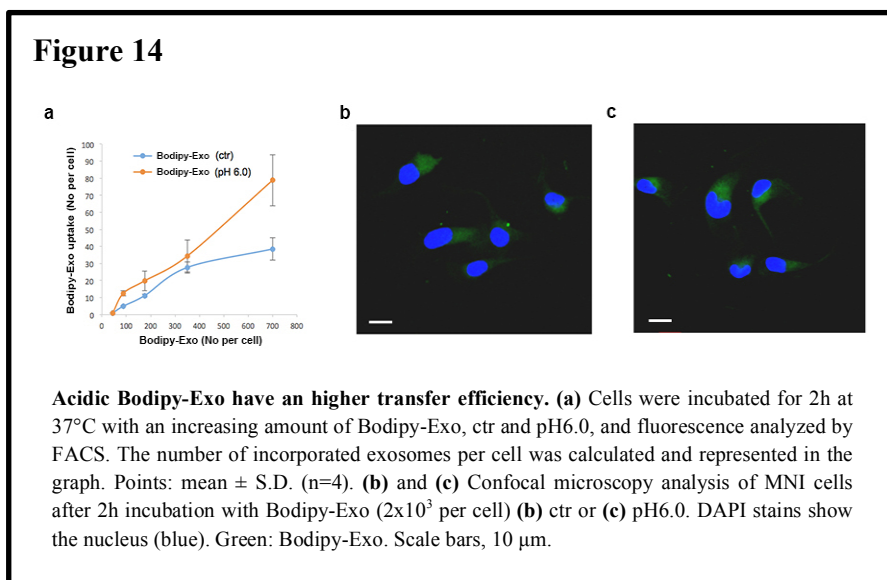
in the MNI acidic pH-responsive (Fig. 13a) and in the MI not responsive cell lines (Fig. 10d). We found that Alix (Fig. 13b) was significantly upregulated after short time pH 6.0 exposure and decreased together with Tsg101 (Fig. 13c) after 24h, thus suggesting the enhanced exosome release as the result of an augmented biosynthesis and following upregulated secretion. Interestingly, these markers were found unchanged during 24h acidic treatment in MI cells (Fig. 13d,e,f), in line with their unresponsiveness to acidic pH. Overall, these findings suggest that melanoma stage is an important parameter for melanoma responsiveness at acidic pHs.



8. Acidic exosomes induces migration and invasion in melanoma cells.

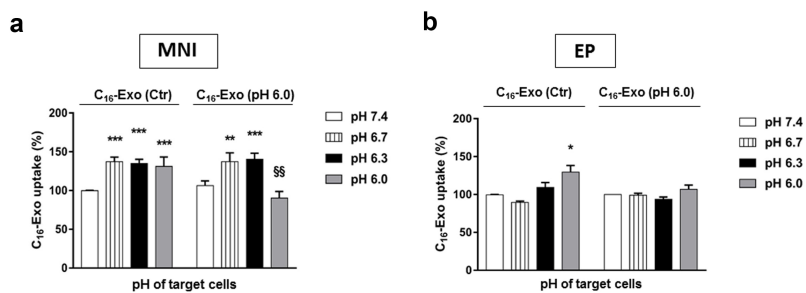
We evaluated whether acidic exosomes could play a role in melanoma progression and studied if they alone were able to transfer migration and invasion capability in control cells. In this set of experiments, we chose pH 6.0 value, because the exosome recovery is very high and used MNI cells for their increased response to acidic pH.

It has already been demonstrated that acidic exosomes display a higher fusion capability with plasma membrane of target cells (Parolini *et al.*, 2009). Thus, we first measured the change in acidic exosomes uptake. Dose-response experiments indicated a higher transfer efficiency of acidic Bodipy-Exo (pH6.0), which was constantly reproduced at increasing vesicle doses (Fig. 14a). Cells treated with fluorescent exosomes were analysed at confocal microscopy to visualize vesicle distribution, and found that both classes of captured exosomes were visible in the cytoplasmic area around nucleus (Fig. 14b,c).



We then wondered if pH culture medium of target cells could influence exosome transfer (Fig. 15). We found that both control and acidic Bodipy-Exo have higher transfer efficiency in acidic extracellular pH, excluding acidic exosome in pH 6.0 medium, that was even lower than control exosome at pH 7.4. This last result may further explain the higher exosome availability in pH 6.0 condition, being the re-uptake on cells decreased with respect to control.

Figure 15

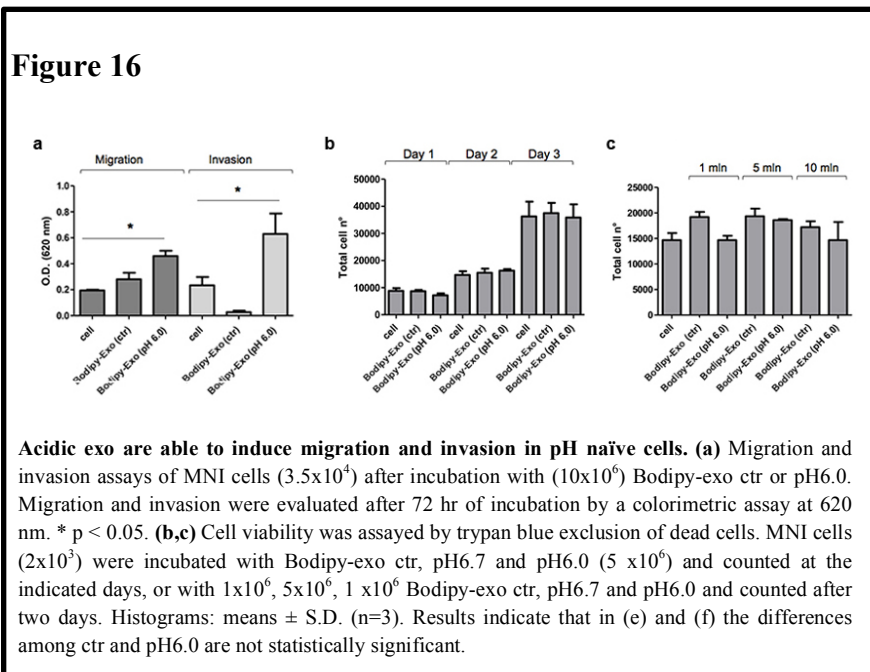


C16-exo uptake at extracellular acid pH. 17×10^6 Bodipy-Exo (ctr) and (pH6.0) obtained from (a) MNI and (b) EP cells, were incubated for 2h at 37°C with parental cells (0.05×10^6) at the indicated pHs. The number of incorporated exosomes per cell was calculated and represented as percentage of respective control at pH 7.4. Points: mean \pm S.D. (n=3) *, $p < 0,05$; **, $p < 0,01$; ***, $p < 0,005$ vs respective pH 7.4 condition; §§, $p < 0,01$ vs C16-exo ctr at pH 7.4

Next, the functional role of these two classes of exosomes was explored through *in vitro* migration and invasion assays (Fig. 16a). MNI melanoma cells were incubated for 72 h with the same amount of exosomes (1×10^7) released from control or pH6.0-cultured cells. The uptake of acidic Bodipy-Exo induced a significant increase in cell migration and invasion, thus we hypothesized that a specific molecular content together with a higher amount of transferred acidic exosomes

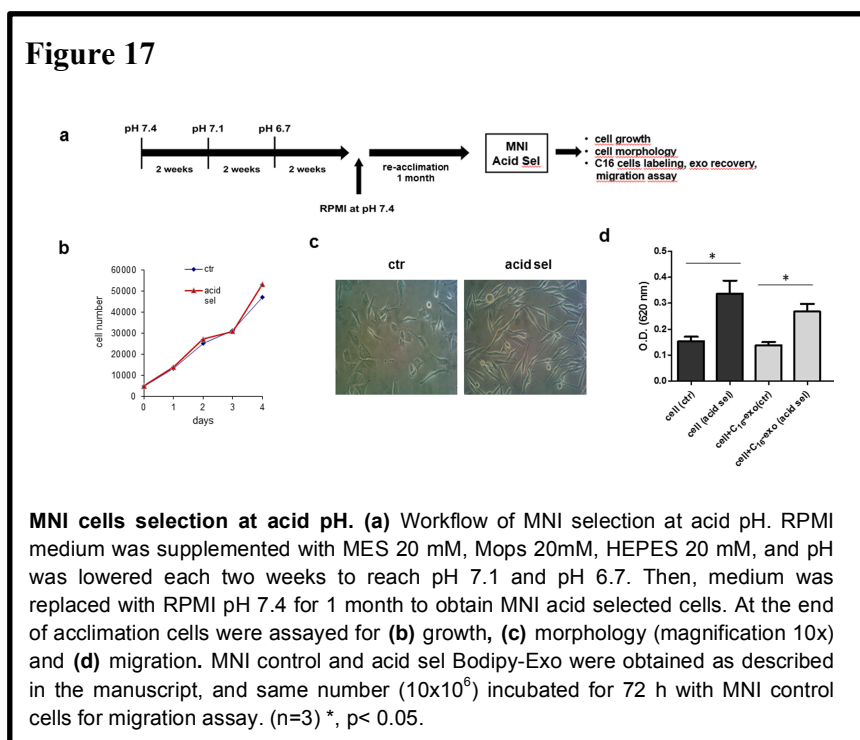
could be responsible of cell acquired aggressiveness. To exclude the enhanced cell migration and invasion as the result of increased cell proliferation, we examined the effects of control and pH6.0 Bodipy-Exo on MNI cell growth. After 72 h incubation, cell proliferation was not affected by exosome treatments either in time (Fig.16b) and dose-response (Fig.16c) experiments.

Altogether, these data highlight the exosome capacity to transmit molecular signals that make cells able to metastasize.



To address whether these results could mirror the *in vivo* process where a slow acclimation at low pH is required to select resistant cells (Moellering *et al.*, 2008), we selected MNI cells for two months, by lowering pH culture medium, followed by 1 month re-acclimation at physiological pH (Fig. 17a). In line with 24 h pH 6.0 treatment, we observed no variation in cell proliferation (Fig. 7b) an elongated cell

morphology (Fig. 17c), and acquired migratory ability in acidic selected condition (Fig. 17d). Remarkably, exosomes obtained from acidic selected cells induced migration in control cells, thus confirming a stable pro-migratory role exerted by acidic microenvironment through exosomes.



9. Acidic exosomes display enrichment in metabolic pathways related to tumor aggressiveness.

Looking for the different molecular cargos potentially responsible for the newly acquired metastatic properties, we investigated the protein composition of exosomes secreted by MNI cells upon acidic treatment by a quantitative mass spectrometry analysis.

Exosomes recovered after 24 h of cell culture at acidic (pH6.0) and control conditions were run on 4-12% SDS-PAGE and subjected to in-gel trypsinization and the extracted peptides were then analyzed by Nano-HPLC. A total number of 186 and 157 proteins were identified in pH6.0 and control samples, respectively.

The fluorescent vesicle preparation were further validated by the presence of 24 (pH6.0) and 21 proteins matching some of the most frequently identified exosome protein markers (http://exocarta.org/exosome_markers) (Table I). Moreover, the lack in our lists of melanosome markers, such as DCT and GPNMB, excluded any possible contamination with melanosomes, which are vesicles containing the pigment melanin and abundantly secreted from melanocytes (Dror *et al.*, 2016).

Table I

Gene	GenBank ID*	Probe name	Mentel-Cox <i>p</i>-value**
HRAS	3265	212983_at	0.010599
IQGAP1	8826	213446_s_at	NS
ACTN1	87	200601_at	NS
ACTN4	81	208636_at	NS
CDC42	998	214230_at	NS

CFL1	1072	1555730_a_at	NS
CFL2	1073	233496_s_at	0.002532
FN1	2335	210495_x_at	NS
NRAS	4893	202647_s_at	0.002301
GSN	2934	202647_s_at	0.044629
VCL	7414	200930_s_at	NS
CD44	960	229221_at	NS
TIMP3	7078	201147_s_at	0.029350
THBS1	7057	201110_s_at	NS
TLN1	7094	203254_s_at	NS
CTNND1	1500	1557944_s_at	NS
ICAM1	3383	215485_s_at	NS
DNAJA2	10294	209157_at	NS
GANAB	23193	214626_s_at	0.003695
HSP90AA1	3320	211968_s_at	NS
HSP90B1	7184	216449_x_at	0.040481

HSP90AB1	3326	200064_at	0.029072
HSPA1L	3305	233694_at	0.048446
HSPA5	3309	230031_at	0.026684
HYOU1	10525	200825_s_at	0.037596
VCP	7415	214990_at	NS

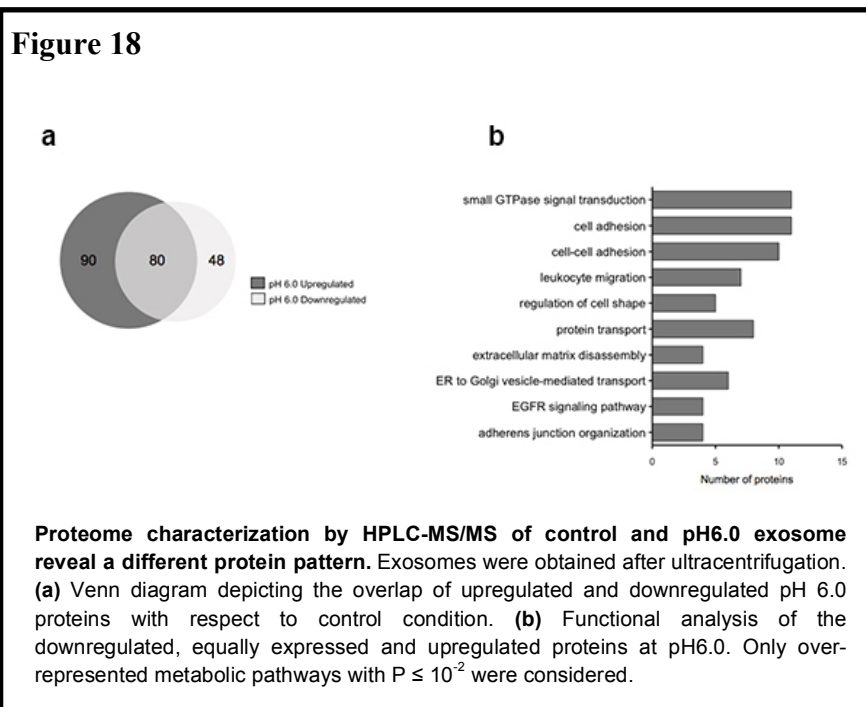
Meta-analysis of upregulated protein in acid exosomes through PrognScan. The analysis was performed by interrogating PrognScan database for gene expression in cancer tissue samples versus overall survival rates of patients with metastatic melanoma. All the listed genes refer to proteins involved in metastatic processes found upregulated in acid exosomes (see Additional Table 3). The analysis has been performed by using the dataset GSE19234, publicly accessible at GEO database (Gene Expression Omnibus database, <https://www.ncbi.nlm.nih.gov/geo>).
* publicly accessible at <https://www.ncbi.nlm.nih.gov/gene>
** Numbers depict Mentel-Cox p values for gene expression with significant difference in patient's overall survival. Only values with $p < 0.05$ are indicated. NS, patient's overall survival not significant ($p \geq 0.05$) for the indicated high or low gene expression.

We found that 24 h incubation at low pH was sufficient to modify exosome protein profile, being more than 50% of the proteins up-regulated, as displayed by the comparative Venn diagram (Fig.18a).

Functional annotation analysis of these three data sets was performed interrogating KEGG pathway database (Fig. 18b).

Taken together, these results show that exosome released at low pH contain specific proteins whose transfer to recipient cells can promote melanoma malignancy.

Interestingly, in acidic conditions, functional categories such as proteoglycans, focal adhesion and protein processing in endoplasmic reticulum, responsible for melanoma migration and invasion, metastasis and survival (Knutson *et al.*, 1996; Hess *et al.*, 2005; Jiang *et al.*, 2007), resulted over-represented.

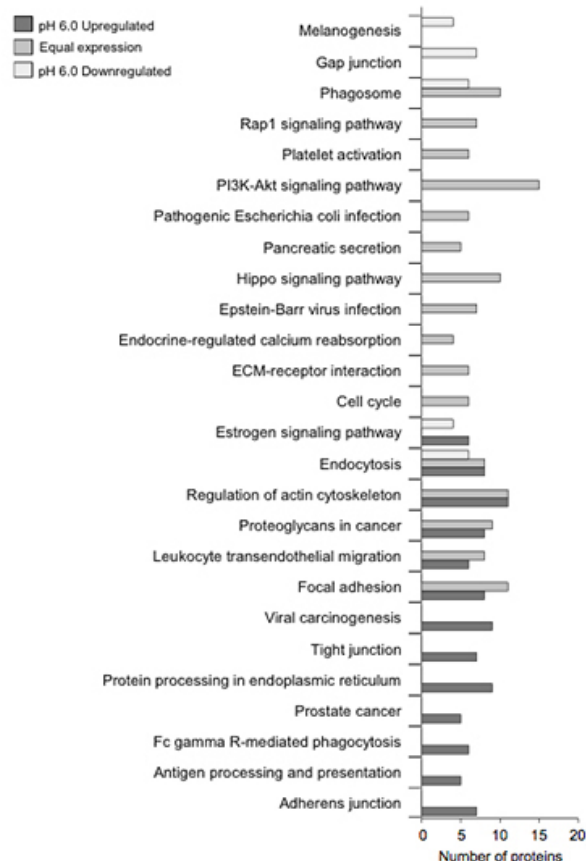


Further analyses by using Gene Ontology (GO, <http://www.geneontology.org>) confirmed the enrichment of acidic pH up-regulated proteins in some key biological processes (Fig.19) as cell-cell adhesion, leukocyte migration, regulation of cell shape, small GTPase mediated signal transduction, EGFR signaling pathways, all associated with the migratory properties of the cells.

10. Acidic exosomes content mirrors protein expression at metastatic site of melanoma patients.

To find a clinical relevance of modified exosome content at acidic pH, we performed a meta-analysis of all the metastasis-related functional

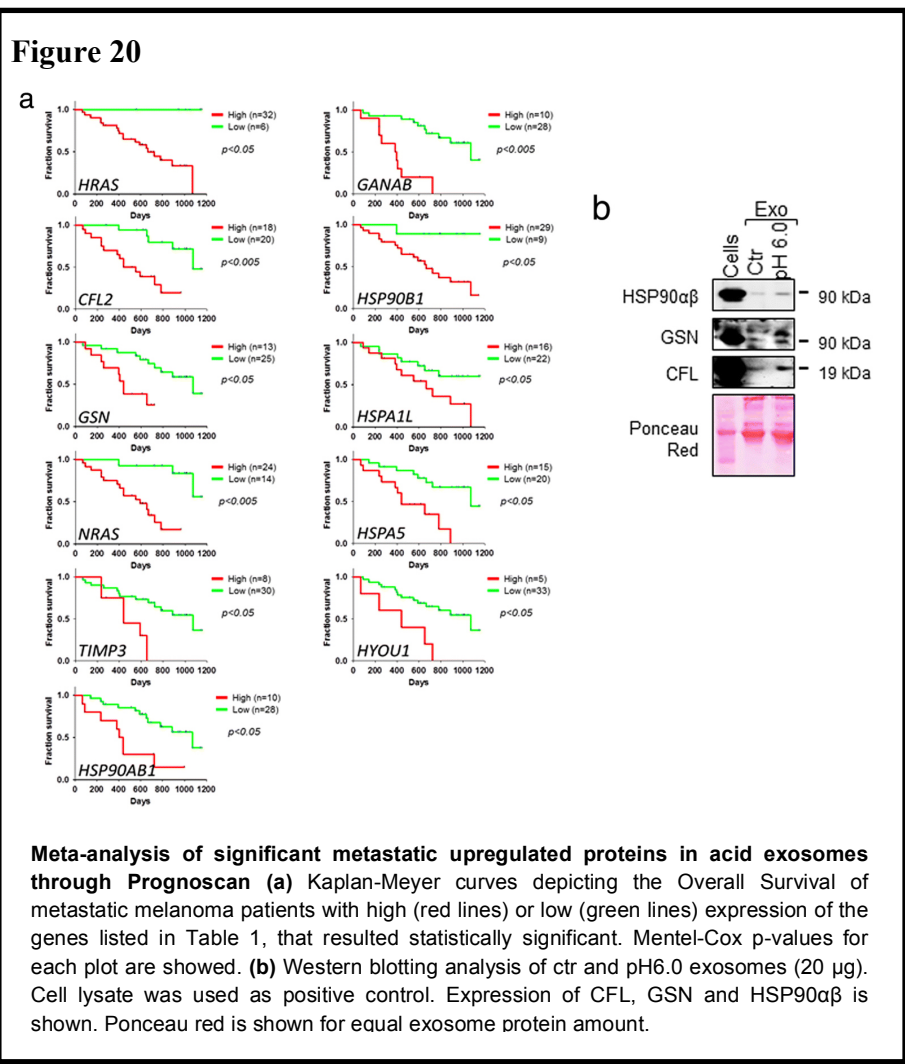
Figure 19



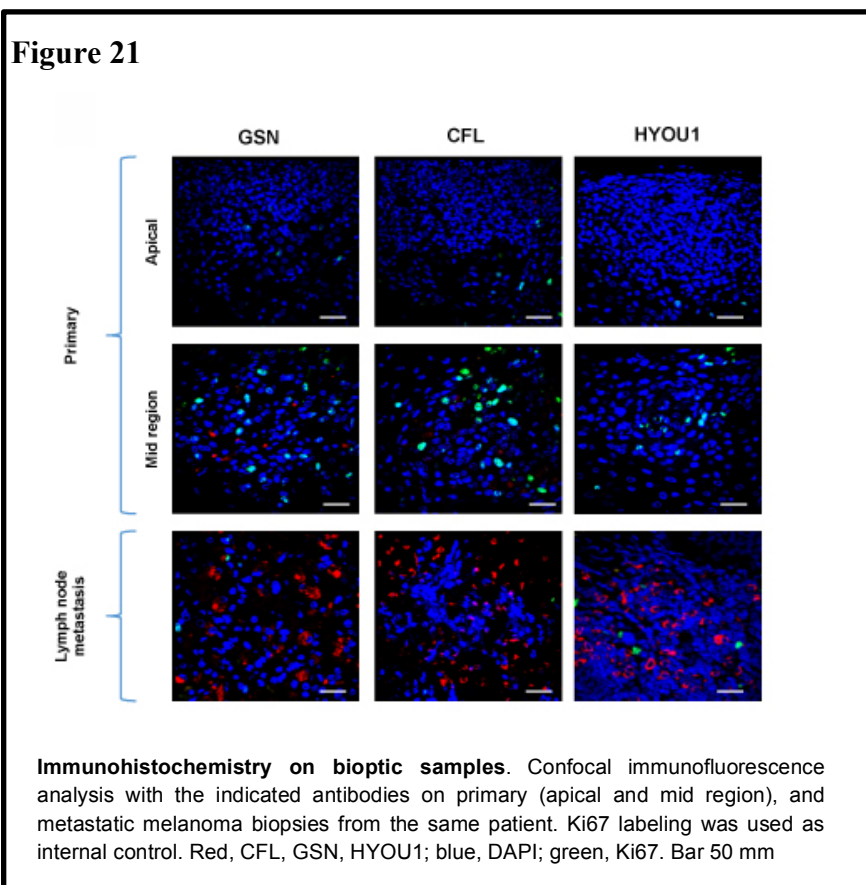
Proteome characterization by HPLC-MS/MS of control and pH6.0 exosome reveal a different protein pattern. GO enrichments of pH6.0 upregulated proteins. Only over-represented categories with $P \leq 10^{-2}$ were considered.

categories, by using Prognoscan database (Mizuno *et al.*, 2009). Interestingly, around 50% of these genes, represented by HRAS, GANAB, CFL2, HSP90B1, HSP90AB1, GSN, HSPA1L, NRAS, HSPA5, TIMP3, HYOU1, showed a positive correlation of their high expression in cancer tissues and poor prognosis in patients with metastatic melanoma (Fig. 20a). These data were further confirmed

analysing by western blot the expression of a representative set of these gene products, i.e. HSP90, CFL2, GSN in exosomes released at acidic pH (Fig. 20b). As expected, the upregulation of all proteins tested was evident in acidic exosomes compared to control.



Finally, the expression levels of CFL, GSN and HYOU1 proteins were evaluated on some representative bioptic samples from melanoma patients (Fig. 21). Interestingly, a general increase in the level of these proteins was observed in lymph node autologous metastases compared with their primary counterparts.



All together, these data demonstrate that acidic exosomes contain molecules representative of the protein profile in metastatic sites of melanoma patients. This may indicate acidic exosomes as a diagnostic tool of poor prognosis in melanoma patients.

DISCUSSION

Exosomes have entirely emerged to be important contributors to cancer biology. They represent important mediators for intercellular communication and are able to modulate recipient cell phenotype and to induce changes in components of the tumor microenvironment, enabling disease progression. Their content, number and size differ under defined microenvironmental conditions, such as those developed during tumor progression (Peinado *et al.*, 2012). Almost all cell types, based upon their physiological state, have the capability to discharge vesicles (Nagarajah, 2016; Gomez *et al.*, 2018). Although too often they are generically named exosomes this nomenclature should be applicable only to intraluminal vesicle whose biogenesis strictly attain the multi-vesicular bodies (MVBs) derivation. This kind of ambiguity comes from an absence of demonstration of their intracellular origin and lack of clearly defined and decisive methods to identify EVs types.

In order to track the intracellular flow linked to exosome biogenesis towards vesicle release, we developed an innovative methodology to metabolically label fluorescent exosomes whose number and fluorescence intensity can be precisely analyzed by Flow Cytometry (FC) (Coscia *et al.*, 2016). The use of conventional FC to identify purified exosomes represented a step forward with respect to the complex instruments previously used for this purpose (Pospichalova *et al.*, 2015).

We observed by TLC analysis that treating cells with the fluorescent palmitic acidic analogue BODIPY FL C₁₆ (Bodipy C₁₆), this is promptly metabolized within the Endoplasmic Reticulum (ER), likely in its smooth portion, into the majority of phospholipid species including the unconventional Bis(monoacylglycero)phosphate (BMP). Importantly BMP, being a specific membrane marker of the MVB and intraluminal vesicles compartments, can discriminate exosomes from microvesicles that are originated from the plasma membrane (Record *et al.*, 2018).

Whereby this methodology embodies an effective strategy to study exosome biogenesis, to monitor their release in the external milieu and to assess their transfer into recipient cells. All in all, by means of experimental procedures such as HPTLC and confocal microscopy we brought into evidence a direct Bodipy FL C₁₆ metabolic lipid flow that starts from ER, goes through late endosomes/intraluminal vesicles formation and terminates in an extracellular release of fluorescent exosomes.

Therefore, in this study, we provide evidence that a population of exosomes can be dynamically tracked over time from the metabolic site of their membrane envelope formation towards extracellular secretion. Moreover, lipid extraction of fluorescent cells and exosome unambiguously demonstrate that the observed intracellular fluorescence was not due to free probe diffusing in the cells, either alone or bound to the BSA used as carrier. Noteworthy, neutral lipid analysis showed that Bodipy C₁₆ is not metabolized to triglycerides or cholesterol esters, lipids specifically secluded in the lipid droplets storage compartment (Pol, Gross and Parton, 2014). These observations are in agreement with previous studies (Louie *et al.*, 2013) where it has been described that tumor cells, primarily metastatic cells and in particular melanoma cells (Kwan *et al.*, 2014), incorporate exogenous palmitate into pathways that generate structural lipids rather than lipids destined to oxidative pathways or lipid droplets (Akoumi *et al.*, 2017). Exclusion of lipid droplets labelling is substantiated by the strong intracellular colocalization of Bodipy fluorescence with Filipin, a stain specific for unesterified cholesterol. On the other hand, exosomes collected at different times of chase show that Bodipy C₁₆ is present almost completely in the form of polar lipids with very little residual free Bodipy C₁₆.

These data are consistent with the notion that the ER forms functional contacts with endosomes (van der Goot and Gruenberg, 2014). Moreover, it has been shown that during their biogenesis endosomes become more tightly associated with the ER (Friedman *et al.*, 2013) and

that one function of ER-endosome contact sites is the transfer of free cholesterol, taken up from plasma membrane, into early endosomes (Rocha *et al.*, 2009). An attractive hypothesis is that fluorescent lipids metabolized in the ER are incorporated into endosomes at the ER/endosomes contact sites, which later undergo intraluminal vesicles formation and maturation into MVB.

To clearly characterize exosome we performed iodixanol density gradient separation and electron microscopy. When exosome pellets were run on iodixanol density gradients and each fraction analysed for Bodipy-Exo content and for exosome markers expression, these experiments revealed that the Bodipy-Exo population separated as a homogenous discrete peak and that the corresponding fractions were positive for exosome markers Flotillin-1, TSG101 and CD81. Moreover, TEM analysis of the iodixanol gradient fractions containing the fluorescent peak showed vesicles of the exosome characteristic size that were positive for Bodipy and CD63. Finally, to further prove fluorescent exosome biogenesis, we treated cells with GW4869, an inhibitor of neutral sphingomyelinase, that is commonly used to block exosome secretion (Li *et al.*, 2013; Wang *et al.*, 2014; Essandoh *et al.*, 2015). Accordingly, we found that this treatment decreases the number of released vesicles, revealing the ceramide-dependent biogenesis of Bodipy-Exo.

Further characterization of Bodipy-Exo was obtained by monitoring by FC the presence of the tetraspanins CD63 and CD81 on fluorescent exosomes. Fluorescent vesicles exhibited colocalization with these exosomal markers, respectively 8% and 14% for CD63 and CD81 which is in fair agreement with previous independent data obtained by others using a more sophisticated FC analysis with dedicated instrument settings (Kormelink *et al.*, 2016).

Moreover, an additional demonstration of the exosomal nature of Bodipy-Exo came from the ability of an antibody against the Bodipy moiety of fluorescent lipids to specifically immunoprecipitate fluorescent vesicles. Here, the use of CFDA-SE (carboxyfluorescein diacetate succinimidyl ester), a fluorescent protein reactive reagent that that is

cleaved of acetate groups by vesicles esterases enzymes to form an amine-reactive fluorescent protein products, confirmed that Bodipy-Exo are intact vesicles, containing a protein cargo. Notably, our results highlight that flotillin-1, whereas co-isolates with exosomes of the same specific floating density, is excluded from the immunoprecipitated fluorescent Exo population, which is in agreement with previous reports showing that flotillin-1 cannot be considered an exosome marker (Kowal *et al.*, 2016). Together, the lines of evidence presented so far strongly suggest that the metabolically labelled fluorescent vesicles population are indeed *bona fide* exosomes.

To fulfil the purpose to determine the kinetic of exosome secretion, we made out pulse-chase experiment. We were able to identify secreted exosomes as soon as 5 minutes after labelling, and a principal secretion peak at 1 hour, that could represent the time needed for MVB to reach the plasma membrane. Importantly, the pulse time does not influences the kinetic of vesicles release, but vary the number of detected vesicles, due to the amount of fluorescent probe absorbed by the cell and so the less intense exosome fluorescent labelling. Therefore, exosome release is independent from probe incorporation, supporting the idea of the existence of a cellular mechanism that organizes such flow.

This exosome labelling strategy allows challenging application to experiments concerning the mechanism underpinning exosome uptake on target cells. In fact by dose-response experiments, we were able to identify among FCS components, BSA, the factor that prevents exosome autologous uptake. The hypothesis is that albumin present in bloodstream can help exosome to preserve its structure and stability enabling these vesicles to reach and be absorbed only by specific target cell. However, this approach represents only the initial step for the study of pathways and molecules involved in the specific recognition and fusion of exosomes on target cells, and for future studies that aim to use exosome as therapeutic tool.

So far, we show that this cell labelling strategy enable the exosome *in vitro* investigation at any stage of their development and in any environmental condition, such as extracellular acidic pH.

During tumor progression, microenvironment is an important and unique platform of cancer biology that is pivotal for either promoting immune tumor rejection or protecting the tumor and promote their progression (Zhang *et al.*, 2017). One aspect of tumor microenvironment is pH fluctuation, which occurs during tumor progression. Then, we applied the above-described methodology to monitor exosome secretion in various microenvironmental pH conditions.

Microenvironmental acidic pH exerts multiple roles in tumor advancement that imply local invasion and dissemination of cancer cell (Robey *et al.*, 2009; Estrella *et al.*, 2013) activation of MMPs (Fiaschi *et al.*, 2013), and impairment of the immune response (Lardner, 2001). In the melanoma model, external low pH was found to promote metastasis (Rofstad *et al.*, 2006) and to affect exosome traffic (Parolini *et al.*, 2009). An exosome functional role in the development of tumor was principally described in the later stages of melanoma progression, being exosomes involved in the production of long-distance metastases (Hood, San and Wickline, 2011). Nonetheless, a role of exosomes in driving metastatic properties, at intratumoral level under acidic pressure, was never defined so far.

We studied a panel of four differently staged human melanoma cell lines, that we described and divided into two group: i.e. BRAF wild type or mutated and with low or high expression of E- and N- cadherin representing epithelial-mesenchymal transition (EMT) process. The analysis of the amount of secreted exosomes in all cell lines, helped us to define an intermediate stage sensitive and responsive to environmental acidic pH. In fact, cells that were responsive to acidic pH induced an enhanced exosome release. Exosomes secreted under this condition have an altered proteomic profile that has the potential to affect the phenotype of target cells, thus inducing migratory and invasive properties on control melanoma cells. It is conceivable that increased exosome release at this stage is crucial for the progression of the disease at a step in which the

maximal spread of newly acquired and specific molecular information are needed to drive and sustain tumor aggressiveness. Notably, changes induced by microenvironmental acidic pH are stable, even after re-acclimation at pH 7.4, as demonstrated by experiments of cells in acidic selection.

In melanoma the correlation between amount of secreted exosomes and disease stage has not yet been completely clarified, being reported in some studies an increased amount of exosomes in plasma from advanced patients (Logozzi *et al.*, 2009; Alegre *et al.*, 2014), and in other studies similar numbers of exosomes in patients at different clinical stages (Hood, San and Wickline, 2011; Lazar *et al.*, 2015). We here found that metastatic melanoma release a higher amount of exosomes than primary melanoma, supporting the idea that the number of secreted vesicles is a hallmark of disease stage.

We here reported that the increase in secreted exosomes is mainly due to a higher vesicles biosynthesis and release in the extracellular space. Investigating the influence of medium pH on exosome transfer, we found that the increased exosome secretion at pH 6.0 may be the result of a reduced re-uptake on target cells. So, these two issues represent some steps probably involved in the mechanism of exosome release and transfer.

Finally, to explore change in exosome protein profile stimulated by pH variations, we carried out a comparative proteomic analysis of exosome secreted under control and acidic conditions. We identified some protein categories upregulated in acidic exosomes, that were interestingly already found related to metastatic processes (Lazar *et al.*, 2015). Due to the different nature of these molecules, we can speculate about independent functional roles occurring in cell transformation, and ultimately leading to enhanced cell aggressiveness.

Nowadays, in melanoma a reliable diagnostic and prognostic significance of exosomes has yet to be demonstrated (Alegre *et al.*, 2016; Tucci *et al.*, 2018). To establish a clinical relevance of exosome protein content, we applied a meta-analysis approach, using PrognoScan

database. We found that in acidic exosomes about 50% of upregulated molecules are correlated with poor prognosis in melanoma patients, that are HRAS, GANAB, CFL2, HSP90B1, HSP90AB1, GSN, HSPA1L, NRAS, HSPA5, TIMP3, HYOU1. Moreover, the relevance of a set these molecules (CFL2, GSN and HYOU1) was confirmed by *ex vivo* experiments on bioptic samples of primary melanoma and autologous lymph-node metastases, (patient with Clark's level IV), whereas Hsp90 protein overexpression was previously described (Huang *et al.*, 2009). Thus, these molecules may represent a melanoma stage specific signature and could be the object of new target therapies against melanoma development. In particular, we can hypothesize a prominent role for GSN and CFL2 in inducing cell migration, through the actin cytoskeleton reorganization, thereby directly modulating the migratory behaviour of melanoma cells.

In conclusion, we here described the key role of transferred vesicles together with their specific content in the regulation of tumorigenic cellular effects, opening the way for future studies focusing on mechanisms interfering with the production, transfer or uptake of acidic exosomes.

Altogether, these findings contribute to a better understanding of the role of exosomes in a specific stage of melanoma progression driven by extracellular acidity. The specific content of exosomes produced under acidic conditions may acquire a prognostic and therapeutic value.

MATERIAL AND METHODS

1. Cell lines

We utilized Me1007 early primary melanoma (EP) and Mel501 metastatic not invasive (MNI) that were obtained by Istituto Nazionale Tumori (Milan, Italy), authenticated according to a standard short tandem repeat-based genotyping at Ospedale Policlinico San Martino (Genova, Italy), and periodically tested for mycoplasma contamination. WM115 primary invasive (PI) and WM266-4 metastatic invasive (MI) are commercially available and, upon arrival, were expanded, frozen and stored under liquid nitrogen.

Mel501 represents a primary low invasive melanoma, WM115 is a primary invasive and WM266-4 an advanced metastatic melanoma. WM115 and WM266-4 were obtained from the same patient.

It might be interesting to evidence that Me1007, and Mel501 carry no classical mutations, whereas the other cell lines are B-RAF mutated (V600D) (Additional file 1). Melanoma cells were cultured in RPMI-1640 or Dulbecco modified Eagle's medium (DMEM) (GIBCO by Life Technologies) supplemented with 10% fetal calf serum (FCS), in a humidified 5% CO₂ incubator.

The culture media at various pHs were obtained as follows. For pH 6.7 condition, we minimized the pH change during the cell culture by addition of 20 mM MOPS (3-(N-morpholino) propanesulfonic acid) to medium containing FBS, then adjusted with HCL 1N to pH 6.7. A stronger acidic condition (pH 6.0) was obtained by the addition of HCL 1N to medium containing FBS, that allowed a cell culture pH fluctuation between 6.0 and 6.3. After 24 h incubation pH was evaluated by pH meter and found unchanged for pH 6.7 condition, whereas in case of pH 6.0 condition ranged between 6.1-6.3.

For long time acidic selection, RPMI medium was supplemented with MES 20 mM, Mops 20mM, HEPES 20 mM. pH was lowered each two weeks to reach pH 7.1 and pH 6.7. Then, medium was replaced with RPMI pH 7.4 for 1 month to obtain MNI acidic selected cells.

The bioptic melanoma specimens used in this study were obtained from the archives of the Istituto Dermopatico dell'Immacolata-IRCCS (Rome-Italy). Signed informed consent was obtained by patients. For each patient, melanoma samples, including primary and autologous metastasis, were analyzed. Sampling and handling of human tissue material were carried out in accordance with the ethical principle of the Declaration of Helsinki.

2. Cell labelling

BODIPY FL C₁₆ fatty acid (Bodipy C₁₆) (Life Technologies) was prepared as described (Coscia *et al.*, 2016). Briefly, one aliquot (100 µL) of 1 mM stock in methanol of Bodipy C₁₆ was dried under nitrogen gas, resuspended with 30 µL of 20 mM KOH, heated for 10 min at 60 °C and finally resuspended in 70 µL PBS containing 2% fatty acid-free bovine serum albumin (FF-BSA, Sigma-Aldrich). MNI and EP cells (50% confluence) were incubated with Bodipy FL C₁₆ (4,4-difluoro-5,7-dimethyl-4-bora-3a,4a-diaza-s-indacene-3-hexadecanoic acid) (C₁₆) (Life Technologies) by addition of 7 µM C₁₆ in medium supplemented with 0.3% FCS (labelling medium) for 5 h at 37 °C. Then, cells were washed with H-BSA, to remove lipid excess, and complete culture medium was added.

Palmitic acid were prepared as described for Bodipy C₁₆. Aliquotes were resuspended in 20mM KOH, PBS 2% FF-BSA and were used for cell culture treatment at a final concentration of 7 µM in cell labelling medium, for 5 h at 37 °C. Cells were washed twice with H-BSA and complete culture medium was added.

Conditioned medium was harvested after 24 hours and processed for exosome isolation or kept at 4 °C up to a week.

3. Cell treatment with GW4869

The nSMase inhibitor, GW4869 (Sigma, USA) was stored at +4 °C as a 5 mM stock suspension in DMSO. For cell culture treatment, the

suspension was diluted into a working solution (10 μ M) in culture medium. Cells were pre-treated with GW4869 or DMSO (ctr) for 19h, and then were labelled with Bodipy C16 for 5 hours at 37 °C in cell labelling medium with GW4869 or DMSO. At the end of the incubation, cells were washed twice and complete medium containing GW4869 or DMSO were added for the indicated times. Conditioned medium was processed for Bodipy-Exo isolation or kept at 4 °C up to a week.

4. Exosome isolation

Conditioned medium was centrifuged at 2,000 \times g for 20 minutes to remove cells and cell debris. Supernatant from previous centrifugation was centrifuged at 10,000 \times g to remove bigger microvesicles. Then, for exosomes isolation, the 10K supernatant was centrifuged at 100,000 \times g (100K) for 3 hours, and pellet was washed in 12 mL of PBS at 100,000 \times g for 3 hours. All ultracentrifugation steps were performed at 4 °C using a SW41 Ti rotor (Beckman Coulter). Exo and MV were stored at 4°C with Protease and Phosphatase Inhibitor Cocktail (Roche) for Exo count and further analysis.

5. Fluorescent labelling of Exosome proteins

To fluorescently label exosome proteins, freshly pelleted vesicles were resuspended in PBS containing 10 μ M of the membrane permeable reagent CFDA-SE (Life Technologies), and incubated for 60 min at RT. Alternatively, external Exo proteins were labelled with 10 μ M of the far-red fluorescent protein reactive dye Alexa Fluor 647 NHS Ester (Succinimidyl Ester) (NHS-AF647, Life Technologies, catalog# A20006) for 30 min at RT (C₁₆/AF647 Exo). At the end of the incubation 10 mM L-Glutamine was added to stop the reaction.

6. Exosome biogenesis

MNI cells cultured to 50% confluency were pulsed with 7 μ M Bodipy C₁₆ for different times at 37 °C in cell labelling medium, washed twice with PBS and chased in fresh complete medium. Conditioned medium was harvested at time intervals, adding at each time point fresh complete medium. The cycle harvest/fresh medium addition was repeated at different time points, as indicated. Exosomes were isolated from conditioned medium by differential ultracentrifugation as described above, counted by flow cytometry (FC) and analysed by western blot for specific Exo markers.

7. Flow Cytometry Analysis and quantification of Exosomes

Flow cytometry (FC) of Bodipy-Exo was performed on a Gallios Flow Cytometer (Beckman Coulter) using an optimized procedure as previously described (Coscia *et al.*, 2016). Briefly, 5 μ L of fluorescent Exo or MV were mixed with 20 μ L of Flow-Count Fluorospheres (Beckman Coulter) and further diluted with PBS to a final volume of 200 μ L. FC analysis was performed by plotting fluorescence at 525/40 nm (FL1) versus log scale side scatter (SSarea). The instrument was set at flux high and the analysis was stopped at 2,000 Flow-Count Fluorospheres events. Fluorescent EVs total number was established according the formula: $x = (((y \times a)/b)/c) \times d$ where y = events counted at 2,000 counting beads; a = number of counting beads in the sample; b = number of counting beads registered (2,000); c = volume of sample analysed; and d = total volume of exosome preparation. Kaluza Software v. 2.0 (Beckman Coulter) was used for FC analysis.

8. Lipids extraction and analysis

Lipid extraction from cells and exosomes was performed according to Folch procedure (FOLCH, LEES and SLOANE STANLEY, 1957).

Briefly, cells and exosomes were resuspended in 1,5 ml H₂O and then 6 ml of Chloroform/Methanol (2:1, v/v) were added. Samples were centrifuged for 15 min at 1.500 x g, upper phase and interphase were discarded and lower phase was dried under N₂ flow. Neutral lipids were separated on silica gel 60 plates (Merck) with a solvent system of hexane/diethyl ether/acetic acid (70:30:1, v/v/v). The zones on silica gel corresponding to phospholipids (PL) were scraped off, extracted with chloroform/methanol (2:1, v/v) and further developed by high-performance thin-layer chromatography (HPTLC) with a solvent system of chloroform/methanol/32% ammonia (65:35:5, v/v/v/v). Fluorescent lipids were visualized by scanning with a Typhoon 9200 scanner (Amersham Biosciences). Non fluorescent lipid standards were detected by staining with 3% copper acetate solution in 8 % phosphoric acid and subsequent heating in an oven for 10 min at 120 °C.

9. Iodixanol density gradient for vesicles separation

Bodipy-Exo in 0.6 mL PBS were loaded on top of a 5-35% (w/v) continuous iodixanol (OptiPrep; Sigma-Aldrich) density gradient prepared in homogenization medium (HM) (0,25 M sucrose, 1 mM EDTA, 10 mM Tris-HCl (pH 7.4)), and centrifuged at 100,000 × g for 16 hours in a SW60 swinging bucket rotor (Beckman Coulter) at 4 °C. After centrifugation, 330 µL fractions were collected and density of each fraction was determined by refractometry.

10. Exosome labelling with antibodies for FC analysis

Antibody labelling of Bodipy-Exo was performed according to (Kormelink *et al.*, 2016). Briefly, Bodipy-Exo pellet was resuspended in 15 µL of PE labeled mouse anti-human CD63 (clone H5C6, BD Biosciences, catalog# 561925), PE labeled mouse anti-human CD81 (clone JS-81, BD Biosciences, catalog# 555676), or with PE labeled isotype controls, for 60 min at RT. To separate the labeled EVs from

antibodies, which will interfere in the FC analysis, a discontinuous iodixanol density gradient was prepared. Antibody labeled Bodipy-Exo were added to 260 μ L of PBS/0.05% BSA, mixed with 1 mL 60% iodixanol stock solution and loaded at the bottom of a SW60 tube (Beckman Coulter). The iodixanol gradient was obtained by overlaying sequentially 0.5 mL 40%, 0.5 mL 30% and 1.8 mL 10% iodixanol solutions, prepared by dilution with HM (0,25 M sucrose, 1 mM EDTA, 10 mM Tris-HCl 7.4). Exosomes floated into the gradient by centrifugation in a SW60 rotor (Beckman Coulter) for 18 hours at 192,000 x g. Gradient fractions of 330 μ L were collected from the top of the tube and analysed by FC. Fraction densities were determined by refractometry.

11. SDS-PAGE and Western blot analysis

Samples were resuspended in Laemmli sample buffer (Bio-Rad), with or without freshly added 50 mM Dithiothreitol (DTT), heated for 10 minutes at 95 °C and analysed by 10 or 12% sodium dodecyl sulphate–polyacrylamide gel electrophoresis (SDS–PAGE) and western blot. For the analysis of fluorescent proteins patterns gels were directly scanned on a Typhoon 9200 gel scanner (Amersham Biosciences). For the analysis of Exo markers gels were transferred to Protran Nitrocellulose membrane (Amersham Biosciences). Membranes were blocked in 5% skimmed milk in TBST (10 mM Tris-HCl pH 8.0, 150 mM NaCl, 0.1% Tween 20) for 1 hour at RT. After incubation, membranes were washed three times in TBST for 10 minutes at RT and incubated with primary antibodies in 5% skimmed milk in TBST overnight at 4 °C. The antibodies used were: mouse anti-TSG101 1:1000 (GeneTex, catalog# GTX70255), rabbit anti-HSP90 1:400 (Santa Cruz, catalog# sc-7947), mouse anti-CD81 1:200 (Santa Cruz, catalog# sc-166029), mouse anti-Flotillin-1 1:1000 (BD Biosciences, catalog# 610821), rabbit anti-CD63 1:1000 (System Biosciences, catalog# EXOAB-CD63A-1), mouse anti-CD9 1:200 (Santa Cruz, catalog# sc-13118), Mouse monoclonal antibody to Alix (3A9 #MA183977, Thermo Scientific, Waltham, MA USA); Mouse

monoclonal antibody to TSG101 (4A10 #GTX70255, GeneTex, Irvine, CA USA); Mouse monoclonal antibody to Calnexin (37/Calnexin #610524, BD Transduction Laboratories, Lexington, KY USA), Rabbit polyclonal antibody to HSP90 α/β (H114 #sc7947, Santa Cruz Biotechnology, Dallas, TX USA), Rabbit polyclonal antibody to Cofilin (#3312, Cell Signaling Thechnology, Leiden, The Netherlands), Goat polyclonal antibody to Gelsolin (N-18 #sc6406, Santa Cruz Biotechnology, Dallas, TX USA), Mouse monoclonal antibody to Tyrosinase (T311 #sc-20035, Santa Cruz, Dallas, TX USA), Rabbit polyclonal antibody to Ap2 α (C-18 #sc-184-R, Santa Cruz, Dallas, TX USA), Mouse monoclonal antibody to E-Cadherin (36/E-Cadherin#610181, BD Transduction Laboratories™, Lexington, KY USA), Rabbit Polyclonal Antibody to N-Cadherin (#NB600-1038, Novus, Littleton, CO USA), Mouse monoclonal antibody to α -Tubulin (B-5-1-2 #T5168, SIGMA-Aldrich, Saint Louis, MO USA).

Membranes were then washed three times in TBST for 10 minutes at RT and incubated with the appropriate horseradish peroxidase-conjugated secondary antibody (Bio-Rad) for 1 hour at RT. Supersignal West Dura chemiluminescent substrate (ThermoScientific) was used to detect the signals. The band intensities of the western blots were quantified using Image J software (NIH).

12. *Electron microscopy.*

For immunolabelling, exosome samples were precipitated undiluted at room temperature for 15 min to grids. Next, blocking with 0.5% bovine serum albumin was performed for 10 min. Labelling with anti-CD63 and anti-CD81 antibodies was carried out for 30 min. Following washing steps, Prot A Au were added and incubated for 15 min. After subsequent phosphate-buffered saline and water wash steps, embedding in 0.3% Uranyl acetate in methyl cellulose was finally performed, followed by electron microscopy analysis of exosomes.

13. Immunoprecipitation.

Freshly pelleted Bodipy Exo (25x10⁷ vesicles) were labelled with 10 μ M Succinimidyl ester Alexa Fluor 647 NHS Ester (Life Technologies) in PBS for 30 minutes at RT (Bodipy/AF647 Exo) and when required with 10 μ M CFDA-SE (Life Technologies) (Bodipy/AF647/CFSE Exo) for 30 minutes at RT. Reaction was blocked with 10 mM Glutamine in PBS. Bodipy, Bodipy/AF647 and Bodipy/AF647/CFSE Exo were then immunoprecipitated by incubating with 10 μ g polyclonal anti-Bodipy FL (Life Technologies, catalog# A-5770) in PBS in a final volume of 0.5 mL for 20 hours at 4°C on a roller mixer. 25 μ L of Protein A/G beads (Pierce) were washed three times with PBS, added to Exo and incubated for 1 hour at 4 °C. Pellets were washed twice with PBS for 10 minutes. Immunoprecipitation supernatants were analysed by FC to determine immunoprecipitation efficiency. Supernatants and pellets were run on a 10% SDS-PAGE for protein pattern analysis on Typhoon 9200 gel scanner (Amersham Biosciences) or analysed for exosome markers by western blot.

14. Confocal Microscopy

For Confocal Laser Scanner Microscopy analysis cells were grown on sterilized coverslips for 24 h. For pulse–chase studies cells were metabolically labelled with 7 μ M Bodipy C₁₆, washed in H-BSA, chased or not in complete medium before fixation with 3% paraformaldehyde (PFA) for 30 min at 4°C, quenched with 10 mM NH₄Cl for 10 min at RT and analyzed. For cholesterol staining, cells were pulsed for 2 hours with 7 μ M Bodipy C₁₆, fixed in 3% PFA and incubated with 0,05 mg/mL Filipin (Sigma-Aldrich, catalog# F9765) in PBS for 1h in the dark. AlexaFluor647-conjugated goat anti mouse (Life Technologies, catalog# A21235) was used as secondary antibody. To stain lysosomes, after a 2 hours pulse with 7 μ M Bodipy C₁₆, cells were fixed in 3% PFA and then incubated with 1 μ M LysoTracker Red DND-99 (Life Technologies,

catalog# L7528) in PBS for 30 min at 37 °C. For colocalization studies cells were pulsed for 2 hours with 7 µM Bodipy C16, permeabilized with 0,01% Triton X-100 for 10 min at RT and incubated with the following antibodies: monoclonal anti-CD63 (ThermoScientific, catalog# MA1-19281); anti-CD81 (ThermoScientific, catalog# MA5-13548) and GM130 (BD Transduction, catalog# 610823); AlexaFluor647-conjugated goat anti mouse (Life Technologies, catalog# A21235) was used as secondary antibody.

Coverslips were mounted on the microscope slide with Vectashield antifade mounting medium containing DAPI (Vector Laboratories, Burlingame, CA). Images were taken by a FV1000 confocal microscope (Olympus, Tokyo, Japan), using a (Olympus) planapo objective 60x oil A.N. 1,42. Excitation light was obtained by a Laser Dapi 408 nm for DAPI, an Argon Ion Laser (488 nm) for C₁₆, a Diode Laser HeNe (561 nm) for Alexa 555 and a Red Diode Laser (638 nm) for Alexa 647. DAPI emission was recorded from 415 to 485 nm, Bodipy C16 emission was recorded from 495 to 550 nm, Alexa 555 emission was recorded from 583 to 628 nm and Alexa 647 from 634 to 750 nm.

Cells treated with Bodipy Exo were fixed with paraformaldehyde (3%) (30 min, 4°C), quenched with 10mM NH₄Cl and mounted on the microscope slide with Vectashield antifade mounting medium containing DAPI (Vector Laboratories, Burlingame, CA).

Images recorded have an optical thickness of 0.4 mm. Signals from different fluorescent probes were taken in sequential scan settings, and colocalization was detected in yellow (pseudocolor). Several fields were analyzed for each labeling condition, and representative results are presented.

15. Mass spectrometry analysis and data processing

Exosomes (8 µg) obtained from ctr or pH6.0-treated MNI cells for 24 h incubation in absence of FCS, were separated on precast 4–12% Bis-Tris Gels (Invitrogen) and stained with Coomassie Colloidal Blue. Each

sample lane was cut into sequential 25 slices. Gel slices were destained in 50 mM $\text{NH}_4\text{CO}_3/\text{CH}_3\text{CN}$ 1:1 and shrunk in acetonitrile. The acetonitrile was removed and the gel particles were dried by centrifugation under vacuum. Proteins were reduced (in 10 mM DTT, 25 mM NH_4CO_3 , for 30 min at 56 °C), shrunk again, and alkylated (55 mM iodoacetamide, 25 mM NH_4CO_3 , for 30 min in the dark at room temperature). Gel pieces were washed in 50 mM $\text{NH}_4\text{CO}_3/\text{CH}_3\text{CN}$ 1:1, shrunk in acetonitrile and dried by centrifugation under vacuum. In-gel digestion was performed by adding 12.5 ng/ μl of trypsin (Promega, Madison, WI) in 25 mM NH_4CO_3 at 37 °C overnight under stirring. Supernatants were directly used for mass spectrometry analysis.

Nano-RPLC was performed using a nano-HPLC 3000 Ultimate (Dionex, Sunnyvale, CA) connected to LTQ-XL linear ion trap (Thermo Fisher). Tryptic digests were firstly loaded on a C18 RP-precolum (300 μm i.d.x5 mm; 5 μm particle size; 100 Å pore size; LC Packings-Dionex.), washed by the loading pump at 20 $\mu\text{L}/\text{min}$ with buffer A (5% ACN, 0.1% FA) for 5 min and then on an homemade 12 cm x 75 μm - i.d. Silica PicoTip (8 \pm 1 μm) column (NewObjective, Ringoes, NJ) packed with C18AQ (5 μm particle size; 200 Å pore size, Michrom Bioresources Inc.) for chromatographic separation. Peptides were eluted at 0.3 $\mu\text{L}/\text{min}$ along a 40 min linear gradient to 60% of buffer B (95% ACN, 0.1% FA) and electrosprayed directly into the mass spectrometer. The acquisition was performed in data-dependent Top5 method, with a minimum signal threshold of 200 counts and dynamic exclusion enabled for 30 sec.

Spectra files were analyzed by Sequest HT search engine with Proteome Discoverer 1.4 (ThermoFisher) against the Uniprot Human Reviewed Protein Database (2014 released version) and decoy database. The Carboamidomethylation of cysteines was specified as fixed modification and the oxidation of methionine was set as variable modification; mass tolerance was set to 1 Da for precursor ion and 0.4 Da for fragment ions and a maximum of two missed cleavages was allowed. The Percolator tool was used for peptide validation based on the q-value and high confidence was chosen, corresponding to a false discovery rate (FDR)

≤1% on peptide-level. Proteins were identified with a minimum of 2 peptides rank=1.

Three independent experiments were performed. We identified in exo (pH6.0) 212, 211 and 217 proteins, and in exo (ctr) 194, 239 and 130 proteins. Only proteins identified with two peptides in at least two experiments were considered, and their abundances were estimated by the normalized emPAInorm values according to $emPAInorm = emPAI / \sum_i emPAI$; where $i = 1, N$ and N is the number of proteins [29]. Reproducibility assessments were carried out in both cases (pH6.0 and control), and the two best correlated experiments (Pearson's correlation higher than 0.8) were considered to calculate the averaged emPAInorm value (186 in pH6.0 and 157 in the control) (see Additional file 3).

The emPAInorm ratio (ρ) between emPAInorm values of proteins identified in pH6 and those identified in the control was calculated. According with the emPAI ratio proteins were classified as up-regulated in pH6.0 ($\rho \geq 1.5$), equally regulated in pH6 and in the control ($0.5 \leq \rho \leq 1.5$) and down-regulated in pH6.0 condition ($\rho \leq 0.5$).

Functional analysis was performed by using the DAVID Bioinformatics Resources 6.8 [30]. Proteins up-, equally and down-regulated were mapped on KEGG pathways separately and over-represented categories ($P \leq 10^{-2}$) were considered.

16. Bodipy-Exo transfer and functional assays

To evaluate Bodipy exo transfer to target cells, increasing amounts (40 to 700 exosome per cell) of exosomes (ctr) and (pH6.0) were added to MNI cells in a 96 well plate in duplicate in 100 μ l RPMI without serum and kept for 2 h at 37 °C in incubator. Then medium was removed, cells PBS-washed, detached and subjected to FC analysis as described (Coscia *et al.*, 2016). Briefly, fluorescence data of Bodipy Exo, cell samples, and QuantumTM FITC-5 MESF (Bangs Laboratories, Inc.) standard curve were acquired and transformed into MESF (Molecules of Equivalent Soluble Fluorophores) using the QuickCal analysis template provided with each QuantumTM MESF lot. Then MESF associated to cells were

converted in number of transferred exosomes according the formula: (cell fluorescence (MESF)-cell autofluorescence (MESF))/ exosome fluorescence (MESF).

Migration and invasion studies were performed according to standard procedures.

Cell migration was assayed, as previously described (Albini *et al.*, 1987), using uncoated cell culture inserts (Corning Costar Corporation, Cambridge, MA). Cells were incubated at 37° C in 5% CO₂, and after 72 hr migration was evaluated by a colorimetric assay (Niu *et al.*, 2002) at 620 nm in a microplate reader (Victor X3, Perkin Elmer). Invasion was evaluated as for chemotaxis on culture inserts previously coated with matrigel. Cell viability was measured by exclusion of dead cells with Trypan Blue Solution (0.4%).

17. Meta-analysis of exosomes molecular cargo (Prognoscan).

Prognoscan is a comprehensive online platform for evaluating potential tumor biomarkers and therapeutic targets.

Based on a large collection of cancer microarray datasets with clinical annotation on GEO databases, Prognoscan is a tool to assess the association between specific gene expression and prognosis in patients with cancer (Mizuno *et al.*, 2009).

We used this online database to validate metastasis-related proteins found upregulated in acidic exosomes with the relative gene expression in cancer tissue samples versus Overall Survival (OS) rates of patients with metastatic melanoma.

18. Immunohistochemical staining

Tissue sections from primary cutaneous and metastatic lymph node melanoma samples embedded in paraffin were dewaxed and rehydrated. For immunolocalization studies slides were first subjected to heat-mediated antigenic retrieval (10 mM Sodium Citrate buffer pH 6.0) and

then to melanin bleaching (warm 10% H₂O₂). Subsequently slides were permeabilized (0.1% Triton X-100 for 10 min) and saturated (3% BSA for at least 2h) at RT. After incubation with primary antibody O/N at 4°C (anti Gelsolin ab75832, 1:100, anti Cofilin-1/2 AP08086PU-S Origene and ORP150/HSP12A NBP1-32140 Novus 1:50) in humidified chamber, slides were incubated with specific fluorophore conjugated secondary antibodies (Alexa Fluor, Molecular Probes Eugene, OR, USA) for 45 min at RT. Ki67 (M7240 Clone MIB-1, Dako) was used as positive immunostaining control. Negative controls were performed by omission of the primary antibody in each experiment. Finally, slides were mounted with SlowFade anti-fade reagent containing DAPI (Molecular Probes, Eugene, OR, USA) and analyzed by Olympus F1000 laser-scanning confocal microscopy (Olympus, Tokyo, Japan).

19. *Statistical analysis*

Differences were statistically evaluated using two-tailed Student's t test. Values were considered significant at $P < 0.05$. All data are expressed as the mean \pm SEM from at least three separate experiments. In some experiments one-way ANOVA multiple comparison analysis with Tukey's post test was used. For OS analysis, Mentel-Cox p-values < 00.5 were considered as statistically significant.

REFERENCES

- Admyre, C., Johansson, S. M., Qazi, K. R., Filén, J.-J., Lahesmaa, R., Norman, M., Neve, E. P. A., Scheynius, A. and Gabrielsson, S. (2007) 'Exosomes with immune modulatory features are present in human breast milk.', *Journal of immunology (Baltimore, Md. : 1950)*. American Association of Immunologists, 179(3), pp. 1969–78.
- Akoumi, A., Haffar, T., Moustjerji, M., Kiss, R. S. and Bousette, N. (2017) 'Palmitate mediated diacylglycerol accumulation causes endoplasmic reticulum stress, Plin2 degradation, and cell death in H9C2 cardiomyoblasts', *Experimental Cell Research*. Academic Press, 354(2), pp. 85–94.
- Albini, A., Iwamoto, Y., Kleinman, H. K., Martin, G. R., Aaronson, S. A., Kozlowski, J. M. and McEwan, R. N. (1987) 'A rapid in vitro assay for quantitating the invasive potential of tumor cells.', *Cancer research*. American Association for Cancer Research, 47(12), pp. 3239–45.
- Alegre, E., Sanmamed, M. F., Rodriguez, C., Carranza, O., Martín-Algarra, S., Gonza'lez, A. and González, Á. (2014) 'Study of Circulating MicroRNA-125b Levels in Serum Exosomes in Advanced Melanoma'. *the College of American Pathologists*, 138(6), pp. 828–832.
- Alegre, E., Zubiri, L., Perez-Gracia, J. L., González-Cao, M., Soria, L., Martín-Algarra, S. and González, A. (2016) 'Circulating melanoma exosomes as diagnostic and prognosis biomarkers', *Clinica Chimica Acta*. Elsevier, 454, pp. 28–32.
- Aubuchon, M. M. F., Bolt, L. J. J., Janssen-Heijnen, M. L. G., Verleisdonk-Bolhaar, S. T. H. P., van Marion, A. and van Berlo, C. L. H. (2017) 'Epidemiology, management and survival outcomes of primary cutaneous melanoma: a ten-year overview', *Acta Chirurgica Belgica*. Taylor & Francis, 117(1), pp. 29–35.
- Baietti, M. F., Zhang, Z., Mortier, E., Melchior, A., Degeest, G., Geeraerts, A., Ivarsson, Y., Depoortere, F., Coomans, C., Vermeiren, E., *et al.* (2012) 'Syndecan–syntenin–ALIX regulates the biogenesis of exosomes', *Nature Cell Biology*. Nature Publishing Group, 14(7), pp.

677–685.

Cheng, Q., Li, X., Wang, Y., Dong, M., Zhan, F. and Liu, J. (2017) ‘The ceramide pathway is involved in the survival, apoptosis and exosome functions of human multiple myeloma cells in vitro’, *Acta Pharmacologica Sinica*. Nature Publishing Group, 6, pp. 1–8.

Cicero, A. Lo, Stahl, P. D., Raposo, G., Schuldiner, M. and Guo, W. (2015) ‘Extracellular vesicles shuffling intercellular messages: for good or for bad This review comes from a themed issue on Cell organelles’, *Current Opinion in Cell Biology*, 35, pp. 69–77.

Colombo, M., Moita, C., van Niel, G., Kowal, J., Vigneron, J., Benaroch, P., Manel, N., Moita, L. F., Théry, C. and Raposo, G. (2013) ‘Analysis of ESCRT functions in exosome biogenesis, composition and secretion highlights the heterogeneity of extracellular vesicles.’, *Journal of cell science*. The Company of Biologists Ltd, 126(Pt 24), pp. 5553–65.

Colombo, M., Raposo, G. and Théry, C. (2014) ‘Biogenesis, Secretion, and Intercellular Interactions of Exosomes and Other Extracellular Vesicles’, *Annual Review of Cell and Developmental Biology*, 30(1), pp. 255–289.

Coscia, C., Parolini, I., Sanchez, M., Biffoni, M., Boussadia, Z., Zanetti, C., Fiani, M. L. and Sargiacomo, M. (2016) ‘Generation, Quantification, and Tracing of Metabolically Labeled Fluorescent Exosomes’, in *Methods in Molecular Biology*. Humana Press, New York, NY, pp. 217–235.

Deatherage, B. L. and Cookson, B. T. (2012) ‘Membrane vesicle release in bacteria, eukaryotes, and archaea: a conserved yet underappreciated aspect of microbial life.’, *Infection and immunity*. American Society for Microbiology (ASM), 80(6), pp. 1948–57.

Demers, A., Samami, S., Lauzier, B., Des Rosiers, C., Sock, E. T. N., Ong, H. and Mayer, G. (2015) ‘PCSK9 Induces CD36 Degradation and Affects Long-Chain Fatty Acid Uptake and Triglyceride Metabolism in Adipocytes and in Mouse Liver’, *Arteriosclerosis, Thrombosis, and Vascular Biology*, 35(12), pp. 2517–2525.

Dror, S., Sander, L., Schwartz, H., Sheinboim, D., Barzilai, A., Dishon, Y., Apcher, S., Golan, T., Greenberger, S., Barshack, I., *et al.* (2016) ‘Melanoma miRNA trafficking controls tumour primary niche

formation’.

Essandoh, K., Yang, L., Wang, X., Huang, W., Qin, D., Hao, J., Wang, Y., Zingarelli, B., Peng, T. and Fan, G.-C. (2015) ‘Blockade of exosome generation with GW4869 dampens the sepsis-induced inflammation and cardiac dysfunction’, *Biochimica et Biophysica Acta (BBA) - Molecular Basis of Disease*. Elsevier, 1852(11), pp. 2362–2371.

Estrella, V., Chen, T., Lloyd, M., Wojtkowiak, J., Cornell, H. H., Ibrahim-Hashim, A., Bailey, K., Balagurunathan, Y., Rothberg, J. M., Sloane, B. F., *et al.* (2013) ‘Acidity generated by the tumor microenvironment drives local invasion.’, *Cancer research*. NIH Public Access, 73(5), pp. 1524–35.

Fiaschi, T., Giannoni, E., Taddei, M. L., Cirri, P., Marini, A., Pintus, G., Nativi, C., Richichi, B., Scozzafava, A., Carta, F., *et al.* (2013) ‘Carbonic anhydrase IX from cancer-associated fibroblasts drives epithelial-mesenchymal transition in prostate carcinoma cells.’, *Cell cycle (Georgetown, Tex.)*. Taylor & Francis, 12(11), pp. 1791–801.

FOLCH, J., LEES, M. and SLOANE STANLEY, G. H. (1957) ‘A simple method for the isolation and purification of total lipides from animal tissues.’, *The Journal of biological chemistry*, 226(1), pp. 497–509.

Friedman, J. R., Dibenedetto, J. R., West, M., Rowland, A. A. and Voeltz, G. K. (2013) ‘Endoplasmic reticulum-endosome contact increases as endosomes traffic and mature.’, *Molecular biology of the cell*. American Society for Cell Biology, 24(7), pp. 1030–40.

Fukamachi, T., Wang, X., Mochizuki, Y., Maruyama, C., Saito, H. and Kobayashi, H. (2013) ‘Acidic environments enhance the inhibitory effect of statins on proliferation of synovial cells’, *International Immunopharmacology*. Elsevier, 17(1), pp. 148–153.

Gomez, C. de la T., Goreham, R. V., Serra, J. J. B., Nann, T. and Kussmann, M. (2018) “‘Exosomics’—A Review of Biophysics, Biology and Biochemistry of Exosomes With a Focus on Human Breast Milk’, *Frontiers in Genetics*. Frontiers Media SA, 9.

Gould, S. J. and Raposo, G. (2013) ‘As we wait: coping with an imperfect nomenclature for extracellular vesicles.’, *Journal of extracellular vesicles*. Taylor & Francis, 2.

Greening, D. W., Gopal, S. K., Xu, R., Simpson, R. J. and Chen, W. (2015) 'Exosomes and their roles in immune regulation and cancer', *Seminars in Cell & Developmental Biology*. Academic Press, 40, pp. 72–81.

Hakulinen, J., Sankkila, L., Sugiyama, N., Lehti, K. and Keski-Oja, J. (2008) 'Secretion of active membrane type 1 matrix metalloproteinase (MMP-14) into extracellular space in microvesicular exosomes', *Journal of Cellular Biochemistry*. Wiley-Blackwell, 105(5), pp. 1211–1218.

Harding, C., Heuser, J. and Stahl, P. (1984) 'Endocytosis and intracellular processing of transferrin and colloidal gold-transferrin in rat reticulocytes: demonstration of a pathway for receptor shedding.', *European journal of cell biology*. Urban und Fischer Verlag GmbH und Co. KG, 35(2), pp. 256–63.

Helmlinger, G., Yuan, F., Dellian, M. and Jain, R. K. (1997) 'Interstitial pH and pO₂ gradients in solid tumors in vivo: high-resolution measurements reveal a lack of correlation.', *Nature medicine*, 3(2), pp. 177–82.

Hess, A. R., Postovit, L.-M., Margaryan, N. V, Seftor, E. A., Schneider, G. B., Seftor, R. E. B., Nickoloff, B. J. and Hendrix, M. J. C. (2005) 'Focal Adhesion Kinase Promotes the Aggressive Melanoma Phenotype', *Cancer Res*, 65(21), pp. 9851–60.

Hong, C.-S., Funk, S., Muller, L., Boyiadzis, M. and Whiteside, T. L. (2016) 'Isolation of biologically active and morphologically intact exosomes from plasma of patients with cancer.', *Journal of extracellular vesicles*. Taylor & Francis, 5, p. 29289.

Hood, J. L., San, R. S. and Wickline, S. A. (2011) 'Exosomes released by melanoma cells prepare sentinel lymph nodes for tumor metastasis.', *Cancer research*. American Association for Cancer Research, 71(11), pp. 3792–801.

Hoshino, A., Costa-Silva, B., Shen, T. L., Rodrigues, G., Hashimoto, A., Tesic Mark, M., Molina, H., Kohsaka, S., Di Giannatale, A., Ceder, S., *et al.* (2015) 'Tumour exosome integrins determine organotropic metastasis', *Nature*, 527(7578), pp. 329–335.

Huang, S. K., Darfler, M. M., Nicholl, M. B., You, J., Bemis, K. G., Tegeler, T. J., Wang, M., Wery, J.-P., Chong, K. K., Nguyen, L., *et al.*

(2009) 'LC/MS-Based Quantitative Proteomic Analysis of Paraffin-Embedded Archival Melanomas Reveals Potential Proteomic Biomarkers Associated with Metastasis', *PLoS ONE*. Public Library of Science, 4(2).

Hurley, J. H. (2008) 'ESCRT complexes and the biogenesis of multivesicular bodies.', *Current opinion in cell biology*. NIH Public Access, 20(1), pp. 4–11.

Jiang, C. C., Chen, L. H., Gillespie, S., Wang, Y. F., Kiejda, K. A., Zhang, X. D. and Hersey, P. (2007) 'Inhibition of MEK sensitizes human melanoma cells to endoplasmic reticulum stress-induced apoptosis.', *Cancer research*. American Association for Cancer Research, 67(20), pp. 9750–61.

Kahlert, C. and Kalluri, R. (2013) 'Exosomes in tumor microenvironment influence cancer progression and metastasis.', *Journal of molecular medicine (Berlin, Germany)*. NIH Public Access, 91(4), pp. 431–7.

Knutson, J. R., Iida, J., Fields, G. B. and McCarthy, J. B. (1996) 'CD44/Chondroitin Sulfate Proteoglycan and α 2 β 1 Integrin Mediate Human Melanoma Cell Migration on Type IV Collagen and Invasion of Basement Membranes', *Molecular biology of the cell*. American Society for Cell Biology, 7(3), pp. 383–396.

Kormelink, T. G., Arkesteijn, G. J. A., Nauwelaers, F. A., van den Engh, G., Nolte-'t Hoen, E. N. M. and Wauben, M. H. M. (2016) 'Prerequisites for the analysis and sorting of extracellular vesicle subpopulations by high-resolution flow cytometry', *Cytometry Part A*, 89(2), pp. 135–147.

Kowal, J., Arras, G., Colombo, M., Jouve, M., Morath, J. P., Primdal-Bengtson, B., Dingli, F., Loew, D., Tkach, M. and Théry, C. (2016) 'Proteomic comparison defines novel markers to characterize heterogeneous populations of extracellular vesicle subtypes', *Proceedings of the National Academy of Sciences*, 113(8), pp. E968–E977.

Kreimer, S., Belov, A. M., Ghiran, I., Murthy, S. K., Frank, D. A. and Ivanov, A. R. (2015) 'Mass-Spectrometry-Based Molecular Characterization of Extracellular Vesicles: Lipidomics and Proteomics', *Journal of Proteome Research*. American Chemical Society, 14(6), pp. 2367–2384.

Kwan, H. Y., Fu, X., Liu, B., Chao, X., Chan, C. L., Cao, H., Su, T., Tse, A. K. W., Fong, W. F. and Yu, Z. L. (2014) 'Subcutaneous adipocytes promote melanoma cell growth by activating the Akt signaling pathway: Role of palmitic acid', *Journal of Biological Chemistry*, 289(44), pp. 30525–30537.

Lane, R. E., Korbie, D., Hill, M. M. and Trau, M. (2018) 'Extracellular vesicles as circulating cancer biomarkers: opportunities and challenges.', *Clinical and translational medicine*. Springer, 7(1), p. 14.

Lardner, A. (2001) 'The effects of extracellular pH on immune function', *Journal of Leukocyte Biology*, 69(4), pp. 522–530.

Lazar, I., Clement, E., Ducoux-Petit, M., Denat, L., Soldan, V., Dauvillier, S., Balor, S., Burlet-Schiltz, O., Larue, L., Muller, C., *et al.* (2015) 'Proteome characterization of melanoma exosomes reveals a specific signature for metastatic cell lines', *Pigment Cell & Melanoma Research*, 28(4), pp. 464–475.

Lee, Y.-S., Kim, S. Y., Ko, E., Lee, J.-H., Yi, H.-S., Yoo, Y. J., Je, J., Suh, S. J., Jung, Y. K., Kim, J. H., *et al.* (2017) 'Exosomes derived from palmitic acid-treated hepatocytes induce fibrotic activation of hepatic stellate cells.', *Scientific reports*. Nature Publishing Group, 7(1), p. 3710.

Li, J., Liu, K., Liu, Y., Xu, Y., Zhang, F., Yang, H., Liu, J., Pan, T., Chen, J., Wu, M., *et al.* (2013) 'Exosomes mediate the cell-to-cell transmission of IFN- α -induced antiviral activity', *Nature Immunology*. Nature Publishing Group, 14(8), pp. 793–803.

Li, N., Rochette, L., Wu, Y. and Rosenblatt-Velin, N. (2018) 'New Insights into the Role of Exosomes in the Heart After Myocardial Infarction', *Journal of Cardiovascular Translational Research*. Springer US, pp. 1–10.

Logozzi, M., De Milito, A., Lugini, L., Borghi, M., Calabrò, L., Spada, M., Perdicchio, M., Marino, M. L., Federici, C., Iessi, E., *et al.* (2009) 'High levels of exosomes expressing CD63 and caveolin-1 in plasma of melanoma patients.', *PloS one*. Public Library of Science, 4(4), p. e5219.

Lötvall, J., Hill, A. F., Hochberg, F., Buzás, E. I., Vizio, D. Di, Gardiner, C., Ghossein, Y. S., Kurochkin, I. V., Mathivanan, S., Quesenberry, P., *et al.* (2014) 'Minimal experimental requirements for definition of extracellular vesicles and their functions: A position statement from the

International Society for Extracellular Vesicles', *Journal of Extracellular Vesicles*.

Louie, E., Chen, X. F., Coomes, A., Ji, K., Tsirka, S. and Chen, E. I. (2013) 'Neurotrophin-3 modulates breast cancer cells and the microenvironment to promote the growth of breast cancer brain metastasis.', *Oncogene*. NIH Public Access, 32(35), pp. 4064–77.

Masyuk, A. I., Masyuk, T. V and Larusso, N. F. (2013) 'Exosomes in the pathogenesis, diagnostics and therapeutics of liver diseases.', *Journal of hepatology*. NIH Public Access, 59(3), pp. 621–5.

Mathivanan, S., Ji, H. and Simpson, R. J. (2010) 'Exosomes: Extracellular organelles important in intercellular communication', *Journal of Proteomics*. Elsevier, 73(10), pp. 1907–1920.

Miller, A. J. and Mihm, M. C. (2006) *Melanoma*.

Mizuno, H., Kitada, K., Nakai, K. and Sarai, A. (2009) 'PrognoScan: a new database for meta-analysis of the prognostic value of genes.', *BMC medical genomics*. BioMed Central, 2, p. 18.

Moellering, R. E., Black, K. C., Krishnamurty, C., Baggett, B. K., Stafford, P., Rain, M., Gatenby, R. A. and Gillies, R. J. (2008) 'Acid treatment of melanoma cells selects for invasive phenotypes', *Clinical & Experimental Metastasis*. Springer Netherlands, 25(4), pp. 411–425.

Momen-Heravi, F., Getting, S. J. and Moschos, S. A. (2018) 'Extracellular vesicles and their nucleic acids for biomarker discovery', *Pharmacology & Therapeutics*. Pergamon.

Nagarajah, S. (2016) 'Exosome Secretion-More than Simple Waste Disposal? Implications for Physiology, Diagnostics and Therapeutics', *Journal of Circulating Biomarkers*.

van Niel, G., Charrin, S., Simoes, S., Romao, M., Rochin, L., Saftig, P., Marks, M. S., Rubinstein, E. and Raposo, G. (2011) 'The tetraspanin CD63 regulates ESCRT-independent and -dependent endosomal sorting during melanogenesis.', *Developmental cell*. NIH Public Access, 21(4), pp. 708–21.

Van Niel, G., D'Angelo, G. and Raposo, G. (2018) 'Shedding light on the cell biology of extracellular vesicles', *Nature Reviews Molecular Cell Biology*, pp. 213–228.

Niu, J., Dorahy, D. J., Gu, X., Scott, R. J., Draganic, B., Ahmed, N. and Agrez, M. V (2002) 'Integrin expression in colon cancer cells is regulated by the cytoplasmic domain of the beta6 integrin subunit.', *International journal of cancer. Journal international du cancer*, 99(4), pp. 529–37.

Nolte-, E. N., van der Vlist, E. J., Aalberts, M., Mertens, H. C., Jan Bosch, B., Bartelink, W., Mastrobattista, E., van Gaal, E. V., Stoorvogel, W., Arkesteijn, G. J., *et al.* (2012) 'Quantitative and qualitative flow cytometric analysis of nanosized cell-derived membrane vesicles', *Nanomedicine: Nanotechnology, Biology, and Medicine*, 8, pp. 712–720.

Palmieri, G., Ombra, M., Colombino, M., Casula, M., Sini, M., Manca, A., Paliogiannis, P., Ascierio, P. A. and Cossu, A. (2015) 'Multiple Molecular Pathways in Melanomagenesis: Characterization of Therapeutic Targets.', *Frontiers in oncology*. Frontiers Media SA, 5, p. 183.

Pan, B. T., Teng, K., Wu, C., Adam, M. and Johnstone, R. M. (1985) 'Electron microscopic evidence for externalization of the transferrin receptor in vesicular form in sheep reticulocytes.', *The Journal of cell biology*. The Rockefeller University Press, 101(3), pp. 942–8.

Parolini, I., Federici, C., Raggi, C., Lugini, L., Palleschi, S., De Milito, A., Coscia, C., Iessi, E., Logozzi, M., Molinari, A., *et al.* (2009) 'Microenvironmental pH Is a Key Factor for Exosome Traffic in Tumor Cells * □ S'.

Peinado, H., Alečković, M., Lavotshkin, S., Matei, I., Costa-Silva, B., Moreno-Bueno, G., Hergueta-Redondo, M., Williams, C., García-Santos, G., Nitadori-Hoshino, A., *et al.* (2012) 'Melanoma exosomes educate bone marrow progenitor cells toward a pro-metastatic phenotype through MET', *Nat Med*, 18(6), pp. 883–891.

Peinado, H., Zhang, H., Matei, I. R., Costa-Silva, B., Hoshino, A., Rodrigues, G., Psaila, B., Kaplan, R. N., Bromberg, J. F., Kang, Y., *et al.* (2017) 'Pre-metastatic niches: organ-specific homes for metastases', *Nature Publishing Group*.

Pol, A., Gross, S. P. and Parton, R. G. (2014) 'Biogenesis of the multifunctional lipid droplet: Lipids, proteins, and sites', *Journal of Cell Biology*, 204(5), pp. 635–646.

Pospichalova, V., Svoboda, J., Dave, Z., Kotrbova, A., Kaiser, K., Klemova, D., Ilkovics, L., Hampl, A., Crha, I., Jandakova, E., *et al.* (2015) 'Simplified protocol for flow cytometry analysis of fluorescently labeled exosomes and microvesicles using dedicated flow cytometer', *Journal of Extracellular Vesicles*, 4, p. 25530.

Punnonen, E.-L., Ryhanen, K. and Marjomaki, V. S. (1998) *At reduced temperature, endocytic membrane traffic is blocked in multivesicular carrier endosomes in rat cardiac myocytes Endocytosis-low temperature block-membrane transport*, *European Journal of Cell Biology*.

Rashed, M. H., Bayraktar, E., Helal, G. K., Abd-Ellah, M. F., Amero, P., Chavez-Reyes, A. and Rodriguez-Aguayo, C. (2017) 'Exosomes: From garbage bins to promising therapeutic targets', *International Journal of Molecular Sciences*, 18(3).

Record, M., Carayon, K., Poirot, M. and Silvente-Poirot, S. (2014) *Exosomes as new vesicular lipid transporters involved in cell-cell communication and various pathophysiologicals*, *Biochimica et Biophysica Acta - Molecular and Cell Biology of Lipids*. Elsevier.

Record, M., Silvente-Poirot, S., Poirot, M. and Wakelam, M. J. O. (2018) 'Extracellular vesicles: lipids as key components of their biogenesis and functions', *Journal of Lipid Research*, 59(8), pp. 1316–1324.

Robey, I. F., Baggett, B. K., Kirkpatrick, N. D., Roe, D. J., Donescu, J., Sloane, B. F., Hashim, A. I., Morse, D. L., Raghunand, N., Gatenby, R. A., *et al.* (2009) 'Bicarbonate increases tumor pH and inhibits spontaneous metastases.', *Cancer research*. NIH Public Access, 69(6), pp. 2260–8.

Robinson, D. G., Ding, Y. and Jiang, L. (2016) 'Unconventional protein secretion in plants: a critical assessment', *Protoplasma*. Springer Vienna, 253(1), pp. 31–43.

Rocha, N., Kuijl, C., Van Der Kant, R., Janssen, L., Houben, D., Janssen, H., Zwart, W. and Neefjes, J. (2009) 'Cholesterol sensor ORP1L contacts the ER protein VAP to control Rab7-RILP-p150Glued and late endosome positioning', *Journal of Cell Biology*. The Rockefeller University Press, 185(7), pp. 1209–1225.

Rofstad, E. K., Mathiesen, B., Kindem, K. and Galappathi, K. (2006) 'Acidic extracellular pH promotes experimental metastasis of human

melanoma cells in athymic nude mice', *Cancer Res*, 66(13), pp. 6699–6707.

Schorey, J. S., Cheng, Y., Singh, P. P. and Smith, V. L. (2015) 'Exosomes and other extracellular vesicles in host-pathogen interactions.', *EMBO reports*. European Molecular Biology Organization, 16(1), pp. 24–43.

Simons, M. and Raposo, G. (2009) 'Exosomes – vesicular carriers for intercellular communication', *Current Opinion in Cell Biology*. Elsevier Current Trends, 21(4), pp. 575–581.

Suesca, E., Alejo, J. L., Bolaños, N. I., Ocampo, J., Leidy, C. and González, J. M. (2013) 'Sulfocerebrosides upregulate liposome uptake in human astrocytes without inducing a proinflammatory response', *Cytometry Part A*. Wiley-Blackwell, 83A(7), pp. 627–635.

Théry, C., Zitvogel, L. and Amigorena, S. (2002) 'Exosomes: composition, biogenesis and function', *Nature Reviews Immunology*. Nature Publishing Group, 2(8), pp. 569–579.

Trajkovic, K., Hsu, C., Chiantia, S., Rajendran, L., Wenzel, D., Wieland, F., Schwille, P., Brugger, B. and Simons, M. (2008) 'Ceramide Triggers Budding of Exosome Vesicles into Multivesicular Endosomes', *Science*, 319(5867), pp. 1244–1247.

Tricarico, C., Clancy, J. and D'Souza-Schorey, C. (2017) 'Biology and biogenesis of shed microvesicles.', *Small GTPases*. Taylor & Francis, 8(4), pp. 220–232.

Tucci, M., Mannavola, F., Passarelli, A., Stefania Stucci, L., Cives, M., Silvestris, F., Stucci, L. S., Cives, M. and Silvestris, F. (2018) 'Exosomes in melanoma: a role in tumor progression, metastasis and impaired immune system activity.', *Oncotarget*. Impact Journals, LLC, 9(29), pp. 20826–20837.

van der Goot, F. G. and Gruenberg, J. (2014) 'Close Encounter of the Third Kind: The ER Meets Endosomes at Fission Sites', *Developmental Cell*. Cell Press, 31(6), pp. 673–674.

Vaupel, P., Kallinowski, F. and Okunieff, P. (1989) 'Blood flow, oxygen and nutrient supply, and metabolic microenvironment of human tumors: a review.', *Cancer research*. American Association for Cancer Research,

49(23), pp. 6449–65.

Vella, L., Sharples, R., Lawson, V., Masters, C., Cappai, R. and Hill, A. (2007) 'Packaging of prions into exosomes is associated with a novel pathway of PrP processing', *The Journal of Pathology*. Wiley-Blackwell, 211(5), pp. 582–590.

Vlasov, A. V., Magdaleno, S., Setterquist, R. and Conrad, R. (2012) 'Exosomes: Current knowledge of their composition, biological functions, and diagnostic and therapeutic potentials', *Biochimica et Biophysica Acta (BBA) - General Subjects*. Elsevier, 1820(7), pp. 940–948.

Wang, X., Huang, W., Liu, G., Cai, W., Millard, R. W., Wang, Y., Chang, J., Peng, T. and Fan, G.-C. (2014) 'Cardiomyocytes mediate anti-angiogenesis in type 2 diabetic rats through the exosomal transfer of miR-320 into endothelial cells', *Journal of molecular and cellular cardiology*. NIH Public Access, 74, p. 139.

WARBURG, O. (1956) 'On the origin of cancer cells.', *Science (New York, N.Y.)*, 123(3191), pp. 309–14.

Wike-Hooley, J. L., Haveman, J. and Reinhold, H. S. (1984) 'The relevance of tumour pH to the treatment of malignant disease.', *Radiotherapy and oncology: journal of the European Society for Therapeutic Radiology and Oncology*, 2(4), pp. 343–66.

Willms, E., Johansson, H. J., Mäger, I., Lee, Y., Blomberg, K. E. M., Sadik, M., Alaarg, A., Smith, C. I. E. I. E., Lehtiö, J., EL Andaloussi, S., *et al.* (2016) 'Cells release subpopulations of exosomes with distinct molecular and biological properties', *Scientific Reports*. Nature Publishing Group, 6(1), p. 22519.

You, Y., Shan, Y., Chen, J., Yue, H., You, B., Shi, S., Li, X. and Cao, X. (2015) 'Matrix metalloproteinase 13-containing exosomes promote nasopharyngeal carcinoma metastasis.', *Cancer science*. Wiley-Blackwell, 106(12), pp. 1669–77.

Zhang, X., Tu, H., Yang, Y., Fang, L., Wu, Q. and Li, J. (2017) 'Mesenchymal Stem Cell-Derived Extracellular Vesicles: Roles in Tumor Growth, Progression, and Drug Resistance', *Stem Cells International*. Hindawi, 2017, pp. 1–12.

Supplementary Material

Supplementary References

1. Colombo MP, Maccalli C, Mattei S, Melani C, Radrizzani M, Parmiani G. Expression of cytokine genes, including IL-6, in human malignant melanoma cell lines. *Melanoma Res.* 1992;2:181-9.
2. Liu XY, Lai F, Yan XG, Jiang CC, Guo ST, Wang CY, et al. RIP Kinase Is an Oncogenic Driver in Melanoma. *Cancer Res.* 2015;75:1736-48.
3. Hoek K, Rimm DL, Williams KR, Zhao H, Ariyan S, Lin A, et al. Expression profiling reveals novel pathways in the transformation of melanocytes to melanomas. *Cancer Res.* 2004;64:5270-82.
4. Marincola FM, Hijazi YM, Fetsch P, Salgaller ML, Rivoltini L, Cormier J, et al. Analysis of expression of the melanoma-associated antigens MART-1 and gp100 in metastatic melanoma cell lines and in in situ lesions. *J Immunother Emphasis Tumor Immunol.* 1996;19:192-205.
5. Bellenghi M, Puglisi R, Pedini F, De Feo A, Felicetti F, Bottero L, et al. SCD5-induced oleic acid production reduces melanoma malignancy by intracellular retention of SPARC and cathepsin B. *J Pathol.* 2015;236:315-25.
6. Monzani E, Facchetti F, Galmozzi E, Corsini E, Benetti A, Cavazzin C, et al. Melanoma contains CD133 and ABCG2 positive cells with enhanced tumourigenic potential. *Eur J Cancer.* 2007;43:935-46.

7. Zimmerer RM, Korn P, Demougin P, Kampmann A, Kokemüller H, Eckardt AM, et al. Functional features of cancer stem cells in melanoma cell lines. *Cancer Cell Int.* 2013;13:78.
8. Smalley KS, Contractor R, Nguyen TK, Xiao M, Edwards R, Muthusamy V, et al. Identification of a novel subgroup of melanomas with KIT/cyclin-dependent kinase-4 overexpression. *Cancer Res.* 2008;68:5743-52.
9. Shields JM, Thomas NE, Cregger M, Berger AJ, Leslie M, Torrice C, et al. Lack of extracellular signal-regulated kinase mitogen-activated protein kinase signaling shows a new type of melanoma. *Cancer Res.* 2007;67:1502-12.
10. Klijn C, Durinck S, Stawiski EW, Haverty PM, Jiang Z, Liu H, et al. A comprehensive transcriptional portrait of human cancer cell lines. *Nat Biotechnol.* 2015;33:306-12.

ABBREVIATIONS

ALIX, ALG-2 interacting protein X; **Bodipy C₁₆**, BODIPY FL C₁₆; **Bodipy-Exo**, exosome labelled with BodipyFL C₁₆; **BMP**, bis(monoacylglyceryl)phosphate; **BSA**, bovine serum albumin; **CHOL**, cholesterol; **CFL**, Cofilin; **EMT**, epithelial-mesenchymal transition; **EP**, early primary melanoma; **ER**, endoplasmic reticulum; **ESCRT**, endosomal sorting complex required for transport; **EV**, extracellular vesicle; **Exo**, exosomes; **FC**, Flow Citometry; **GANAB**, glucosidase II alpha subunit; **GSN**, Gelsolin; **H-BSA**, hank's balanced salt solution supplemented with BSA; **HPTLC**, High Performance Thin Layer Chromatography; **HRAS**, HRas proto-oncogene; **HSP90AB1**, heat shock protein 90 alpha family class B member; **HSPA5**, heat shock protein family A member 5; **HSPAIL**, heat shock protein family A member I like; **HYOU1**, hypoxia up-regulated; **IHC**, immunohistochemistry; **ILV**, intraluminal vesicles; **MI** metastatic invasive melanoma; **MNI**, metastatic non invasive melanoma; **MVE**, multi vesicular endosome; **MV**, microvesicles; **NHS-AF647**, AlexaFluor647-conjugated Succinimidyl Ester; **NRAS**, neuroblastoma RAS oncogene; **PE**, phosphatidylethanolamine; **PI**, primary invasive melanoma; **PI**, phosphatidylinositol; **PS**, phosphatidylserine; **TAG**, triacylglycerol; **TIMP3**, Timp metalloproteinase inhibitor 3; **TSG101**, tumor susceptibility gene 101.

List of publications

- Boussadia, Z., Lamberti, J., Mattei, F., Pizzi, E., Puglisi, R., Zanetti, C., Pasquini, L., Fratini, F., Fantozzi, L., Felicetti, F., *et al.* (2018) ‘Acidic microenvironment plays a key role in human melanoma progression through a sustained exosome mediated transfer of clinically relevant metastatic molecules.’, *Journal of experimental & clinical cancer research : CR*. BioMed Central, 37(1), p. 245.
- Zanetti, C., Gallina, A., Fabbri, A., Parisi, S., Palermo, A., Fecchi, K., Boussadia, Z., Carollo, M., Falchi, M., Pasquini, L., *et al.* (2018) ‘Cell propagation of cholera toxin CTA ADP-ribosylating factor by exosome mediated transfer’, *International Journal of Molecular Sciences*, 19(5).
- Coscia, C., Parolini, I., Sanchez, M., Biffoni, M., Boussadia, Z., Zanetti, C., Fiani, M. L. and Sargiacomo, M. (2016) ‘Generation, Quantification, and Tracing of Metabolically Labeled Fluorescent Exosomes’, in *Methods in Molecular Biology*. Humana Press, New York, NY, pp. 217–235.